PRESENTED BY

INTERFERENCE TECHNOLOGY®

2018 COMPONENTS & MATERIALS GUIDE

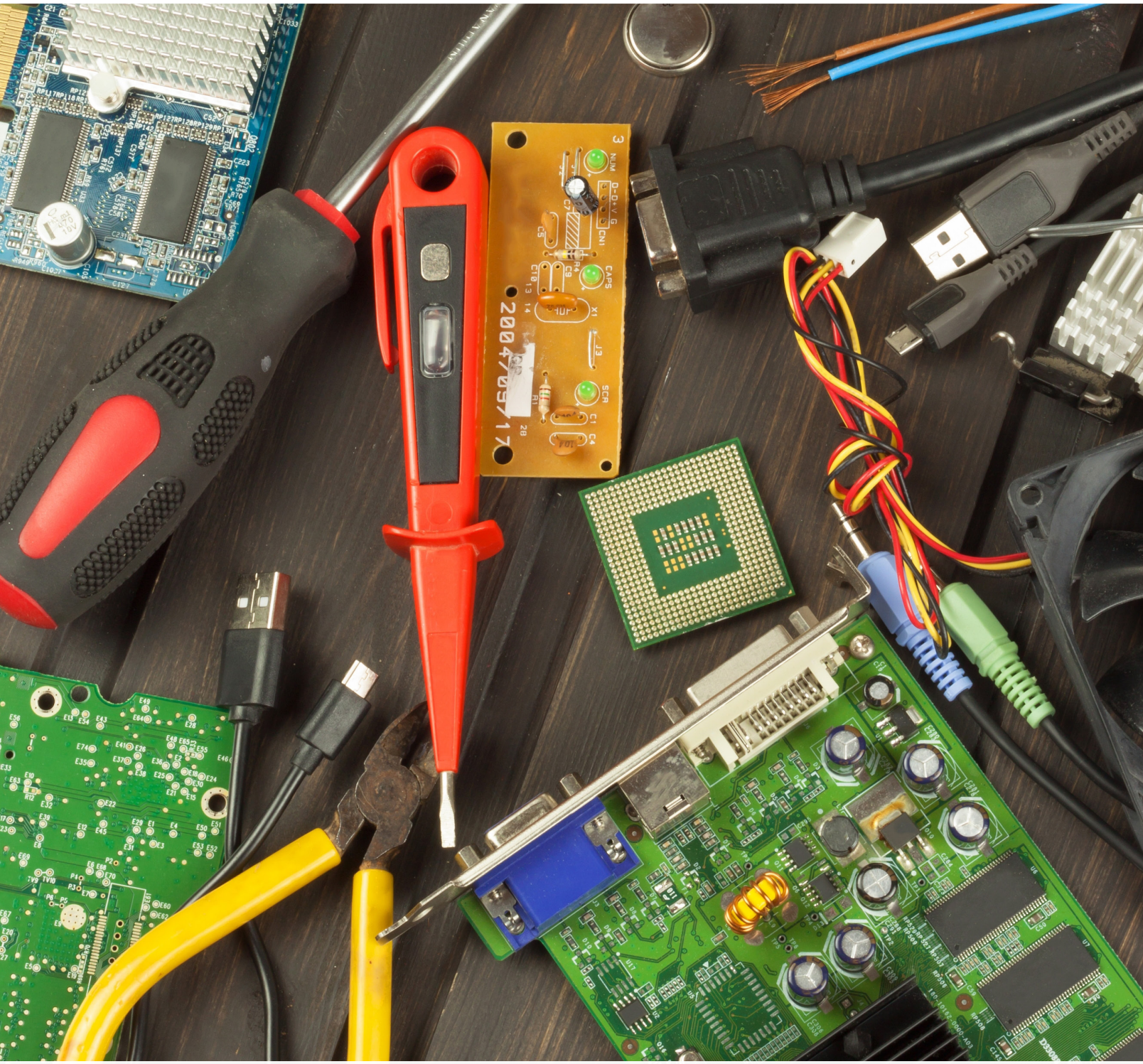

Providing Solutions for EMC Compliance

SCHAFFNER
shaping electrical power

www.schaffnerusa.com

52 Mayfield Avenue | Edison, NJ 08837 | 800-367-5566

TABLE OF CONTENTS

Having an EMC Compliance

EMERGENCY?

YOU need to make the RIGHT CALL!

1.914.806.8063

Quick turnarounds, custom solutions and one-on-one support from the industry's top EMI Filter designers and engineers.

ITG | **The Source for EMI FILTER and COMPONENT Solutions!**

Better products from

The AUTHORITY on EMI FILTERS

www.ITG-Electronics.com/category/2

Engineering Electronics Partnership since 1963

SHIELDING MANUFACTURERS GUIDE

A Guide to Suppliers of EMI Shielding

Your quick reference guide to shielding manufacturers by shielding type, from absorbers to vent panels. Also includes popular gasketing materials such as silicon, form-in-place, finger stock, and various types of board level shields. Contact links are included for convenience.

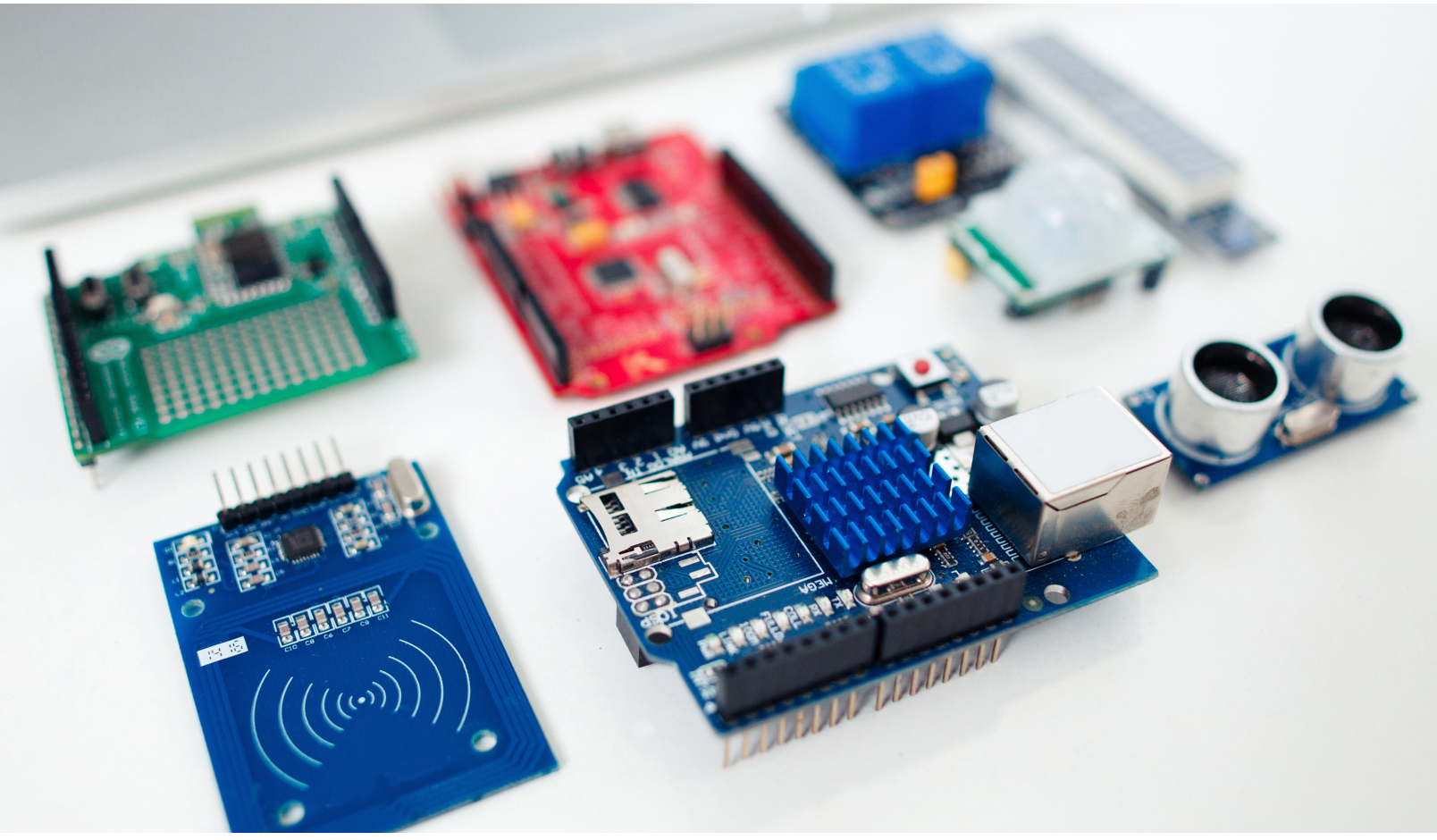

Shielding Manufacturers Guide		Type of Shielding Available																										
Manufacturer	Contact Information - URL	Absorbers	Adhesives	Board Level Shields	Cable Shielding	Conductive Coatings	Coil Springs	Elastomers	Electroless Plating	Fabric over Foam	Ferrites	Fingerstock	Foams	Form in Place	Gaskets	Grease	Grounding Components	Honeycomb Filters	Knitted Wire Mesh	Laminates	Metallized Fabric	High Mu Materials	Sealants	Silicone Elastomers	Tapes	Vent Panels	Windows
3M	www.3m.com	X																							X		
Alco Technologies	www.alcotech.com				X										X				X							X	
ARC Technologies	arc-tech.com	X																									
Bal Seal Engineering Inc.	www.balseal.com						X																				
Fotofab	www.fotofab.com			X					X																		
Ja-Bar Silicone Corp.	ja-bar.com							X																	X	X	
Kemet	www.kemet.com										X																
Kemtron	www.kemtron.co.uk	X		X				X		X	X	X		X						X					X	X	X
Kitagawa Industries America, Inc.	kgs-ind.com	X			X						X				X		X								X		
Laird Technologies	www.lairdtech.com	X	X	X				X		X	X	X		X	X				X	X					X	X	
Leader Tech	leadertechinc.com	X		X	X			X		X	X	X	X	X	X		X	X	X		X	X		X	X	X	
Magnetic Shield Corp.	www.magnetic-shield.com				X																	X					
MAJR Products	majr.com	X		X				X		X	X	X		X	X					X					X	X	X
MAST Technologies	www.masttechnologies.com	X																									
Metal Textile Corp.	www.metexcorp.com	X						X		X		X			X										X	X	X
Nolato Silikonteknik	www.nolato.com					X		X						X	X		X							X			
Orbel	www.orbel.com			X								X									X						
Parker/Chomerics	www.chomerics.com	X	X	X		X										X	X			X			X		X	X	X
Photofabrication Engineering Inc.	www.photofabrication.com			X																							
Rogers Corp.	www.rogerscorp.com							X							X									X			
Schlegel Electronic Materials	www.schlegelemi.com							X		X		X	X												X	X	X
Seleco	seleco.com					X																					
Shielding Source	shieldingsource.com	X						X		X		X	X														
Spira Manufacturing Corp.	www.spira-emi.com														X											X	
SSP Inc.	www.sspinc.com							X																			
Stockwell Elastomerics	www.stockwell.com							X							X			X					X				
Swift Textile Metalizing LLC	www.swift-textile.com																				X						
Tech Etch	www.tech-etch.com			X				X		X		X			X											X	
V Technical Textiles / Shieldex US	www.vtechtextiles.com																				X						
VTI Vacuum Technologies, Inc.	www.vactecinc.com								X					X													
W.L. Gore & Associates	www.gore.com			X											X		X										
Wurth Elektronik	www.we-online.com										X																

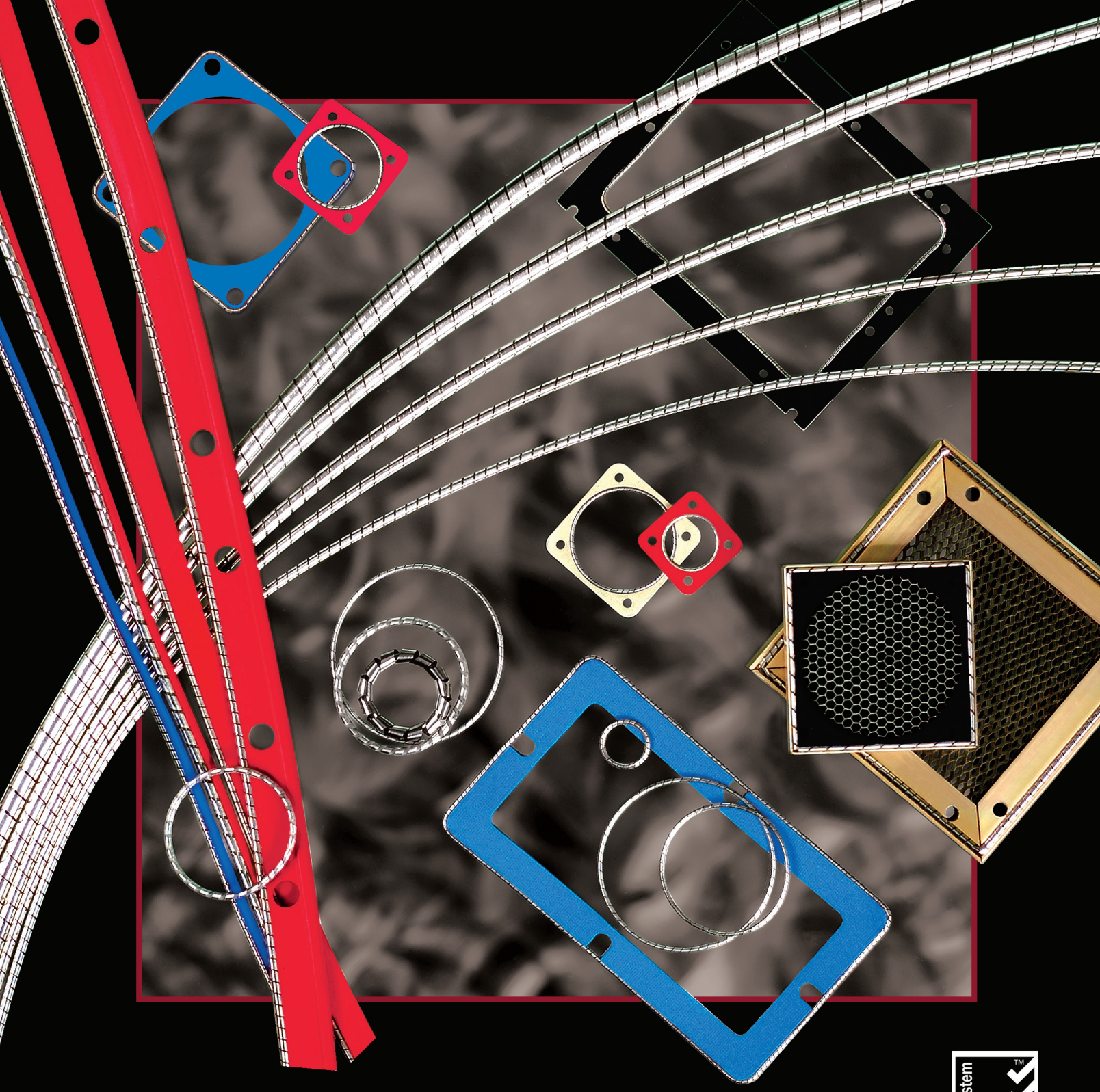

The Inspiration in EMI Shielding

Certified System™

ISO 9001
AS9100

Visit our Website to request Free Samples, an EMI Educational DVD, Technical Assistance, & NEW EMI Shielding Catalog & Design Guide.

www.spira-emi.com

Spira™

(818) 764-8222 info@spira-emi.com

All Products Made in the USA

EMC FILTERS MANUFACTURERS GUIDE

Kenneth Wyatt
Sr. Technical Editor Interference Technology

A Guide to Suppliers of EMI Filters

Your quick reference guide by various EMC filter types. The listing includes AC and DC line filters, filters for chambers, feedthrough, board level, coaxial, ferrite, filtered connectors, power converter, EMP/HEMP, TEMPEST, and custom. Applications include commercial, military, medical, and industrial. Also includes contact links for suppliers.

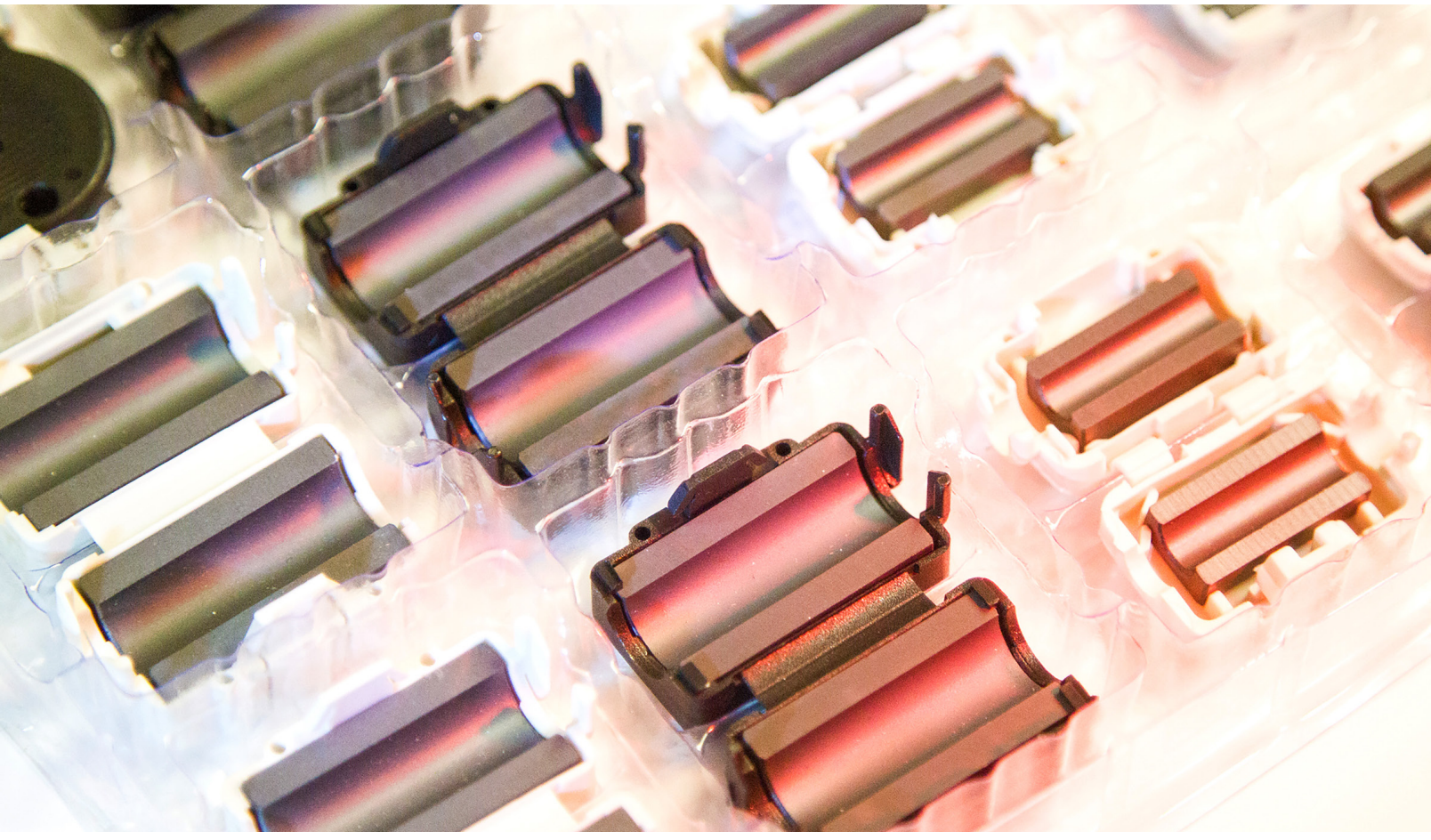

EMC Filters Manufacturers Guide		Type of Filters Available																						
Manufacturer	Contact Information - URL	AC Line	Board Level	Coaxial	Commercial	Common Mode, Power	Custom	DC Line	EMC Chamber	EMP / HEMP / IEMP	Feedthrough	Feedthrough Capacitors	Ferrite Filters	Filtered Connectors	Filter Connector Inserts	Inductors	Industrial	Medical	Military/Aerospace	Power Converter	Signal / Data	Tempest	Tunable	Variable Speed Drive
Americor	www.americor-usa.com	X			X		X											X	X					
Amphenol	www.amphenol.com													X					X		X			
API Technologies	http://eis.apitech.com	X	X	X	X	X	X	X		X	X	X		X		X	X	X	X	X	X			
Astrodyne (LCR & Radius Power)	www.astrodynetdi.com	X			X													X	X					
Block USA	www.block.eu/en_IN/products/emc-filter	X			X												X							
Capcon	www.capconemi.com			X			X		X								X		X					
Captor Corporation	www.captorcorp.com						X			X	X					X	X		X		X	X		
Coilcraft	www.coilcraft.com		X		X	X		X								X				X	X			
Curtis	www.curtisind.com	X			X			X									X	X	X	X				X
Delta Products Corporation	www.deltaww.com	X	X		X	X					X					X	X				X			
EMI Filter Company	www.emifiltercompany.com							X			X	X							X			X		
EMI Solutions	www.4emi.com				X		X							X	X		X		X					
Emitech Micro Components	www.emitech.co.in	X	X		X												X							
EMP-Tronic	www.emp-tronic.se									X														
ETS LINDGREN	www.ets-lindgren.com								X	X											X			
Genisco	www.genisco.com				X		X		X								X				X			
Heilind (Corcom, Deutsch, TE Connect.)	www.te.com	X			X		X							X			X		X		X			
Jiangsu	www.wemctech.com				X				X		X						X							
K&L	www.klmicrowave.com			X																			X	
Kemet	www.kemet.com	X			X				X		X						X	X						X
Knowles (Syfer)	www.knowlescapacitors.com/syfer		X				X	X			X	X			X			X	X		X			
Mini-Circuits	www.minicircuits.com/homepage/homepage.html			X																				
MPE Limited (in EU)	www.mpe.co.uk	X					X	X	X	X	X								X		X	X		
Murata	www.murata.com	X	X		X	X		X					X			X					X			
OnFilter	www.onfilter.com	X					X	X																X
Qualtek	www.qualtekusa.com/products-emi-filters.php	X			X													X						
Quell	www.quell.com			X	X		X							X	X		X	X	X					
Schaffner	www.schaffnerusa.com	X	X		X	X		X			X	X				X	X	X						X
Schurter	www.schurter.com	X														X								
TDK, EPCOS	www.usa.epcos.com	X	X		X	X		X	X		X	X	X			X					X			
TriMag	www.curtisind.com	X			X			X									X	X	X	X				X
WEMS Electronics	www.wems.com						X		X	X	X			X					X		X	X		
Wurth Elektronik	www.we-online.com/web/en/wuerth_elektronik/start.php				X	X		X					X			X				X	X			

Have you tried our Common Mode Choke Finder?

There's nothing common about it!

Search and compare hundreds of common mode choke options in four easy steps.

Step 1: Search parts by Impedance, Attenuation or Inductance at your operating frequency.

Step 2: View results in a sortable table with complete performance specifications and select parts for further analysis.

Step 3: Make direct comparisons of up to six components on single impedance and attenuation graphs.

Step 4: Request free samples of the most interesting parts for evaluation and testing.

It's that Simple!

Give it a test drive at **coilcraft.com/CMCfinder.**

coilcraftdirect.com
No min order. Next day delivery.

Coilcraft®

WWW.COILCRAFT.COM

CLASSICAL SHIELDING THEORY VS. NEAR-FIELD MEASUREMENTS

Bogdan Adamczyk
adamczyb@gvsu.edu

Nick Dipisa
nickdipisa@gmail.com

Abstract
This article addresses the fundamental concepts underlying the classical shielding theory based on Schelkunoff's equations [1]. In order to assess the applicability of these equations, an understanding of their origin, assumptions made in their derivations, and their limitations, are needed. This tutorial article addresses each of these points. The goal is not to show the derivations but to explain the process leading to the final Schelkunoff's equations underlying the accepted shielding theory. The validity of these equations is assessed by performing the magnetic and electric field measurements in the near field of the source. It is shown that the H-field measurements in the near field correlate with the results of the Schelkunoff's equations. The E-field measurements in the near field, however, do not. Instead, the measurement results of the electric field in the near field of the source adhere to the wave theory developed for the far field. A plausible explanation of this fact is that the shielding theory was developed under the assumption of a point source, which is not the case for practical sources and near field measurements.

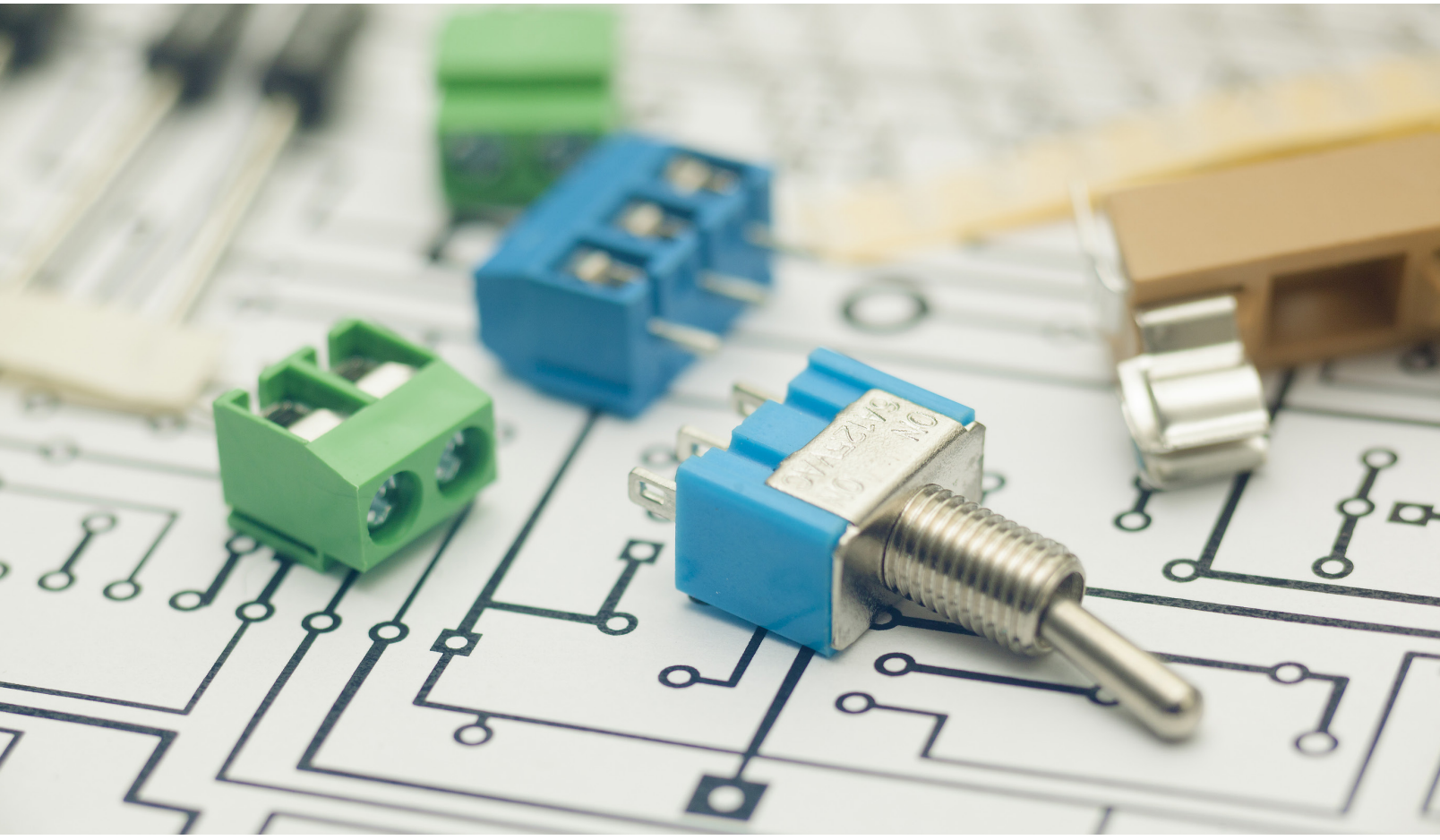

CLASSICAL SHIELDING THEORY VS. NEAR-FIELD MEASUREMENTS

Introduction

Shielding theory is based on three fundamental concepts:

- reflection and transmission of electromagnetic waves at the boundaries of two media,
- radiated fields of the electric and magnetic dipole antennas,
- wave impedance of an electromagnetic wave.

The first concept leads to the analytical formulas for the *far field* shielding effectiveness of a metallic shield in terms of the reflection loss, R, and the absorption loss, A, as functions of frequency, *f* [2], [3]:

$$A_{dB} = 3.34t\sqrt{f\mu_r\sigma_r} \quad (1.1a)$$

$$R_{m,dB} = 14.57 + 10\log_{10}\left(\frac{fr^2\sigma_r}{\mu_r}\right) \quad (1.1b)$$

where *t* represents the thickness of the shield in inches, and μ_r, and σ_r, are the relative permeability (with respect to free space) and relative conductivity (with respect to copper), respectively. These formulas hold for both the electric field shielding and the magnetic field shielding, commonly referred to as the electromagnetic field (or wave) shielding.

When combined with the concepts of the fundamental dipole antennas and wave impedance, the far field formulas lead to the expressions for the *near field* shielding effectiveness.

The absorption loss in the near field is given by the same formula as in the far field, i.e., *Eq. (1.1a)*. The formulas for the reflection loss for the electric field sources and magnetic field sources are different. In the near field, the reflection losses for the electric field sources, R_e, and the magnetic field sources, R_m, are specified by

$$R_{e,dB} = 322 + 10\log_{10}\left(\frac{\sigma_r}{\mu_r f^3 r^2}\right) \quad (1.2a)$$

$$R_{m,dB} = 14.57 + 10\log_{10}\left(\frac{fr^2\sigma_r}{\mu_r}\right) \quad (1.2b)$$

This tutorial article outlines the derivation of Schelkunoff's equations and tests their validity against the near-field measurements. The paper is organized as follows. *Section 1* reviews the reflection and transmission of electromagnetic waves at boundaries between two media. The effect of a metallic shield on the wave transmission is discussed in *Section 2*. Radiated fields of an electric and magnetic dipoles are described in *Section 3*. Far field and near field shielding formulas are presented in *Section 5* and *Section 6*, respectively. In *Section 7* the measurement setup is shown. In *Section 8* the analytical and simulation results are correlated with the near field measurements.

Section 1 – Reflection and Transmission of Electromagnetic Waves at Boundaries

Consider a *normal incidence* of a *uniform plane wave* on the boundary between two media, as shown in *Fig. 1.1*. Each medium is described by three constitutive parameters: μ - permeability, ε – permittivity, and σ – conductivity (note: these are real quantities). It is assumed that each medium is *simple* i.e., linear, homogeneous, and isotropic).

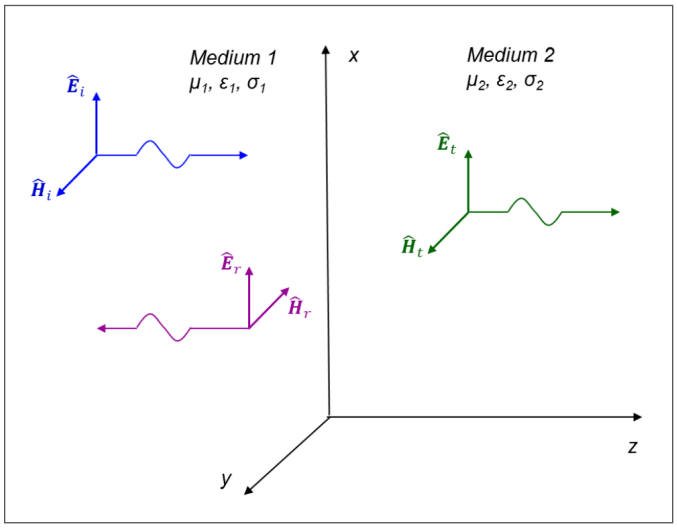

Figure 1.1: Reflection and transmission of a uniform wave at the boundary

When the incident wave encounters the boundary between two media (*xy* plane), a reflected wave and a transmitted wave are created. Imposing the boundary conditions on the electric and magnetic fields at the interface results in the formulas relating the amplitudes of these waves. These amplitudes are related by the complex intrinsic impedances of each medium. The intrinsic impedances are related to the constitutive parameters of the medium and are given by (note: a "hat" above a variable denotes a complex quantity), [3]:

$$\hat{\eta}_1 = \sqrt{\frac{j\omega\mu_1}{\sigma_1 + j\omega\varepsilon_1}} = \eta_1\angle\theta_{\eta 1} \quad (1.3a)$$

$$\hat{\eta}_2 = \sqrt{\frac{j\omega\mu_2}{\sigma_2 + j\omega\varepsilon_2}} = \eta_2\angle\theta_{\eta 2} \quad (1.3b)$$

The amplitude of the reflected wave is related to the incident-wave amplitude by [4]:

$$\hat{E}_r = \hat{\Gamma}\hat{E}_i \quad (1.4a)$$

where $\hat{\Gamma}$ is the reflection coefficient at the boundary, and is given by

$$\hat{\Gamma} = \Gamma\angle\theta_\Gamma = \frac{\hat{E}_r}{\hat{E}_i} = \frac{\hat{\eta}_2 - \hat{\eta}_1}{\hat{\eta}_2 + \hat{\eta}_1} \quad (1.4b)$$

The amplitude of the transmitted wave is related to the incident-wave amplitude by

$$\hat{E}_t = \hat{T}\hat{E}_i \quad (1.5a)$$

where $\hat{\Gamma}$ is the transmission coefficient at the boundary, and is given by

$$\hat{T} = T\angle\theta_T = \frac{\hat{E}_t}{\hat{E}_i} = \frac{2\hat{\eta}_2}{\hat{\eta}_2 + \hat{\eta}_1} \quad (1.5b)$$

Now, consider a metallic shield in the *far field* of the source; the shield has thickness t and surrounded on both sides by air (free space), as shown in *Fig. 1.2*.

The free-space regions are described by the phase constant, β_0, and intrinsic impedance, η_0, given by

$$\beta_0 = \omega\sqrt{\mu_0\varepsilon_0} \quad (1.6a)$$

$$\eta_0 = \sqrt{\frac{\mu_0}{\varepsilon_0}} \quad (1.6b)$$

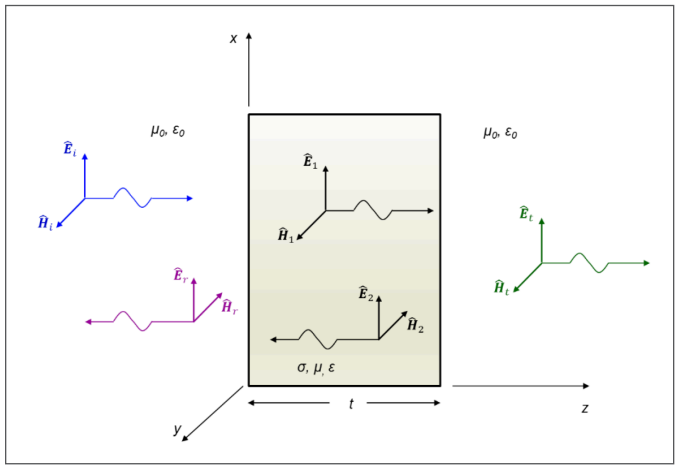

Figure 1.2: Electromagnetic wave impinging on a shield

The shield is described by the propagation constant, $\hat{\gamma}$, and the intrinsic impedance, $\hat{\eta}$, given by

$$\hat{\gamma} = \sqrt{j\omega\mu(\sigma + j\omega\varepsilon)} = \alpha + j\beta \quad (1.7a)$$

$$\hat{\eta} = \sqrt{\frac{j\omega\mu}{\sigma + j\omega\varepsilon}} \quad (1.7b)$$

Upon the arrival at the shield, the uniform plane wave, $(\hat{E}_i,\hat{H}_i)$ is partially reflected, $(\hat{E}_r,\hat{H}_r)$, and partially transmitted, $(\hat{E}_1,\hat{H}_1)$, through the shield. The portion of the incident field that is reflected at the shield interface will be described (in *Section 3*) by the *reflection loss*, R.

The portion of the wave that crosses the shield surface is attenuated as it travels through the shield will be described (in *Section 3*) by the absorption loss, A. The transmitted wave, $(\hat{E}_1,\hat{H}_1)$, upon arrival at the rightmost boundary will be partially reflected, $(\hat{E}_2,\hat{H}_2)$, and partially transmitted, $(\hat{E}_t,\hat{H}_t)$ through the shield.

The reflected wave, $(\hat{E}_2,\hat{H}_2)$, propagates back through the shield towards the first interface, incident from the right. Once again, a portion of this wave is transmitted through the left interface and a portion is reflected and travels to the right. This process continues, but the additional reflected and transmitted waves are progressively attenuated. The portion of the wave that undergoes multiple reflections within the shield will be described (in *Section 5*) by the multiple reflection loss, M.

Section 2 – Electric and Magnetic Field Transmission through the Shield Boundaries

It is very instructive to analyze the effect of the shield on the electric and magnetic fields at the left and right boundaries. The results shown in this section are normally derived under the following assumptions: the shield is thick, made of a good conductor, and located in the far field of the source. The far field assumption translates into the fact the E field impinging onto the shield is perpendicular to the shield. Thus, it is reasonable to argue that the far field results should apply in the near field, as long as the impinging E field is perpendicular to the shield. It is conceivable, therefore, to postulate that some of the electric field lines emanating from practical sources (not point sources) are indeed perpendicular to the surface of the source and thus perpendicular to the shield in the near field. Consequently, to some extent, the far field results should be applicable in the near field. This is indeed the case as we will show in the measurement section.

The space free regions on either side of the shield have the intrinsic impedance specified by *Eq. (1.6b)* and the shield has the intrinsic impedance given by *Eq. (1.7b)*. The assumption of a good conductor results in the following inequality

$$\hat{\eta} << \eta_0 \quad (2.1)$$

This inequality has very important and revealing impact on the magnitudes of the transmitted fields at the shield boundaries. Let's look at the electric field first. At the left boundary the transmission coefficient is [3]

$$\frac{\hat{E}_1}{\hat{E}_i} = \frac{2\hat{\eta}}{\eta_0 + \hat{\eta}} \cong \frac{2\hat{\eta}}{\eta_0}, \quad \hat{\eta} << \eta_0 \quad (2.2)$$

Thus, the electric field transmission coefficient is very small at the first boundary. This means that very little of the electric field is transmitted through the first boundary; that is, *almost all of the incident electric field is reflected*.

This is a very important observation! The consequence of this fact is that (as long as the shield is made of a good conductor) a metallic shield will almost entirely reflect the impinging electric field, regardless of the shield thickness. We will confirm this observation in the measurement section.

Now, let's look at the magnetic field transmission. At the left boundary the transmission coefficient is

$$\frac{\hat{H}_1}{\hat{H}_i} \cong \frac{2\eta_0}{\eta_0 + \hat{\eta}} \cong 2, \quad \hat{\eta} << \eta_0 \tag{2.3}$$

Thus, at the first boundary the transmitted magnetic field doubles. This, again is a very important observation. The consequence of it is that *we need thick shields to attenuate magnetic fields*, and thus the shield thickness matters. We will confirm this observation in the measurement section.

Section 3 – Radiated Fields of the Electric and Magnetic Dipole Antennas

Electric (or Hertzian) dipole, shown in *Fig. 3.1*, is modeled as a very short current element of length *l*, carrying a constant current I_0. The current element is positioned symmetrically at the origin of the coordinate system and oriented along the z axis.

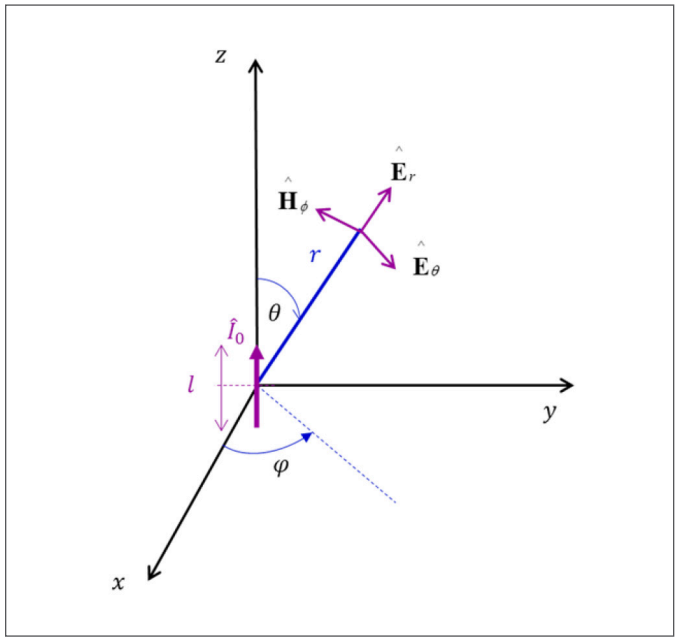

Figure 3.1: Electric (Hertzian) dipole antenna

Electric-dipole total radiated fields are given by [3], [4]:

$$\hat{H}_\phi = \frac{I_0 l}{4\pi}\beta_0^2 \sin\theta\left(j\frac{1}{\beta_0 r} + \frac{1}{\beta_0^2 r^2}\right)e^{-j\beta_0 r} \tag{3.1a}$$

$$\hat{E}_r = 2\frac{I_0 l}{4\pi}\eta_0\beta_0^2 \cos\theta\left(\frac{1}{\beta_0^2 r^2} - j\frac{1}{\beta_0^3 r^3}\right)e^{-j\beta_0 r} \tag{3.1b}$$

$$\hat{E}_\theta = \frac{I_0 l}{4\pi}\eta_0\beta_0^2 \sin\theta\left(\frac{j}{\beta_0 r} + \frac{1}{\beta_0^2 r^2} - \frac{j}{\beta_0^3 r^3}\right)e^{-j\beta_0 r} \tag{3.1c}$$

Magnetic dipole, shown in *Fig. 3.2*, is modeled as a very small loop of radius *a*, carrying a constant current I_0. The loop is positioned symmetrically in the *xy* plane with its center at the origin of the coordinate system.

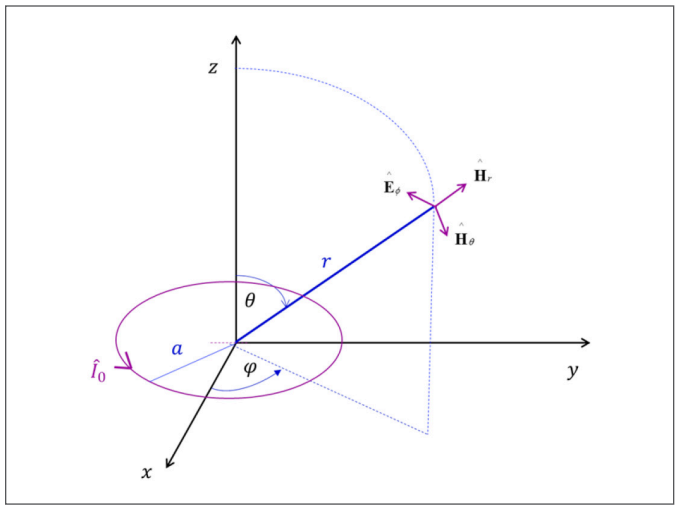

Figure 3.2: Magnetic dipole antenna

Magnetic-dipole radiated fields are given by [3]:

$$\hat{E}_\phi = -j\frac{\omega\mu_0 I_0 a^2 \beta_0^2}{4}\sin\theta\left(j\frac{1}{\beta_0 r} + \frac{1}{\beta_0^2 r^2}\right)e^{-j\beta_0 r} \tag{3.2a}$$

$$\hat{H}_r = j2\frac{\omega\mu_0 I_0 a^2 \beta_0^2}{4\eta_0}\cos\theta\left(\frac{1}{\beta_0^2 r^2} - j\frac{1}{\beta_0^3 r^3}\right)e^{-j\beta_0 r} \tag{3.2b}$$

$$\hat{H}_\theta = j\frac{\omega\mu_0 I_0 a^2 \beta_0^2}{4\eta_0}\sin\theta\left(j\frac{1}{\beta_0 r} + \frac{1}{\beta_0^2 r^2} - j\frac{1}{\beta_0^3 r^3}\right)e^{-j\beta_0 r} \tag{3.2c}$$

It is interesting to note the duality between the field expressions for both dipole antennas. We will use the above expressions for the total radiated fields in the next section, when introducing the concept of the wave impedance.

In many practical applications it is often useful to focus on the near field- and far field radiated fields (instead of the total radiated fields). In the near field, we have

$$\beta r < 1 \quad \Rightarrow \quad \frac{1}{\beta r} < \frac{1}{(\beta r)^2} < \frac{1}{(\beta r)^3} \tag{3.3a}$$

while in the far field, the opposite inequality holds

$$\beta r > 1 \quad \Rightarrow \quad \frac{1}{\beta r} > \frac{1}{(\beta r)^2} > \frac{1}{(\beta r)^3} \tag{3.3b}$$

The boundary between the near and far fields is when

$$\beta r = 1 \quad \Rightarrow \quad r = \frac{1}{\beta} = \frac{1}{2\pi/\lambda_0} = \frac{\lambda_0}{2\pi} \tag{3.4}$$

or

$$r = \frac{\lambda_0}{2\pi} \cong \frac{1}{6}\lambda_0 \tag{3.5}$$

We will refer to this important result in the next section (in *Fig. 4.1*). Utilizing the inequalities (3.3) in the equations for the total radiated fields of the electric and magnetic dipoles leads to the following observations.

In the *near field of the electric dipole* the magnitudes of the fields are primarily influenced as

$$E \sim \frac{1}{r^3}, \quad H \sim \frac{1}{r^2} \tag{3.5a}$$

while in the *near field of the magnetic dipole* the magnitudes are dominated by the mirror expressions

$$E \sim \frac{1}{r^2}, \quad H \sim \frac{1}{r^3} \tag{3.5b}$$

In the far field, of *both the electronic and magnetic dipoles* we have

$$E \sim \frac{1}{r}, \quad H \sim \frac{1}{r} \tag{3.6}$$

Figure 4.1 of the next section contains these important observations.

Section 4 – Wave Impedance

The concept of the wave impedance, when combined with the expressions for the radiated fields in the previous section, leads to the shielding effectiveness formulas.

The electric dipole wave impedance is defined as

$$\hat{Z}_{w,e} = \frac{\hat{E}_\theta}{\hat{H}_\phi} \tag{4.1a}$$

where, $\hat{E}_\theta$ and $\hat{H}_\phi$ are given by *Eqs. (3.1c)* and *(3.1a)*, respectively. The magnetic dipole wave impedance is defined by the dual expression as

$$\hat{Z}_{w,m} = \frac{\hat{E}_\phi}{\hat{H}_\theta} \tag{4.1b}$$

where, $\hat{E}_\phi$ and $\hat{H}_\theta$ are given by *Eqs. (3.2a)* and *(3.2c)*, respectively.

Utilizing *Eqs. (3.1)* and *(3.2)* in *Eqs. (4.1)* leads to the following expressions for the wave impedances. For the electric dipole we have

$$\hat{Z}_w = \frac{\hat{E}_\theta}{\hat{H}_\phi} = \eta_0 \frac{1 - \left(\frac{2\pi r}{\lambda_0}\right)^2 + j\left(\frac{2\pi r}{\lambda_0}\right)}{-\left(\frac{2\pi r}{\lambda_0}\right)^2 + j\left(\frac{2\pi r}{\lambda_0}\right)} \tag{4.2a}$$

while for the magnetic dipole we obtain

$$\hat{Z}_w = \frac{\hat{E}_\phi}{\hat{H}_\theta} = -\eta_0 \frac{\left(\frac{2\pi r}{\lambda_0}\right) + j\left(\frac{2\pi r}{\lambda_0}\right)^2}{\left(\frac{2\pi r}{\lambda_0}\right) + j\left[\left(\frac{2\pi r}{\lambda_0}\right)^2 - 1\right]} \tag{4.2b}$$

When the expressions in *Eq. (4.2)* are evaluated at a distance

$$r = 3\lambda_0 \tag{4.3}$$

the result for the *magnitude of the wave impedance for both the electric and magnetic field* is [3], [4]

$$\left|\hat{Z}_w\right| \cong \eta_0 \tag{4.4}$$

This is why, for the these types of antennas, the far field begins at a distance $r = 3\lambda_0$.

Substituting *Eqs. (3.1c)* and *(3.1a)* into *Eq. (4.1a)* and evaluating it in the near field of an electric dipole gives the wave-impedance magnitude as

$$\left|\hat{Z}_w\right| = \frac{\eta_0}{\beta_0 r} \tag{4.5}$$

We will use this important result when discussing near-field shielding in the next section. Note that in the *very near field*, where, $\beta_0 r \ll 1$, the magnitude of the electric dipole wave impedance is much greater than the intrinsic impedance of free space, i.e.,

$$\left|\hat{Z}_w\right| >> \eta_0 \tag{4.6}$$

This is why, the electric dipole is often referred to as a high-impedance source. Substituting *Eqs. (3.2a)* and *(3.2c)* into *Eq. (4.1b)* and evaluating it in the near field of a magnetic dipole gives the wave-impedance magnitude as

$$\left|\hat{Z}_{w,m}\right| = \eta_0 \beta_0 r \tag{4.7}$$

This important result will be used in the next section. Note that in the *very near field*, where, $\beta_0 r \ll 1$, the magnitude of the magnetic dipole wave impedance is much smaller than the intrinsic impedance of free space, i.e.,

$$\left|\hat{Z}_{w,e}\right| << \eta_0 \tag{4.8}$$

This is why, the magnetic dipole is often referred to as a low-impedance source. The results of this section are often shown in the well-known summary, shown in *Fig. 4.1*.

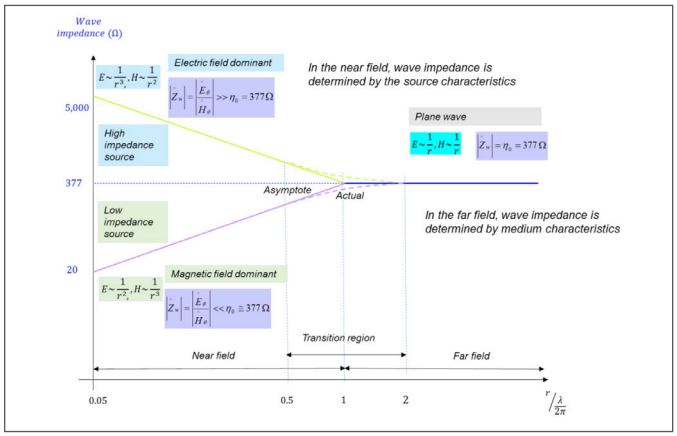

Figure 4.1: Wave impedance as a function of the distance from the source

Section 5 – Far-Field Shielding

The effectiveness of the shield, SE, can be viewed as the ratio of the transmitted-field amplitude to the incident-field amplitude. This ratio is obtained by applying the boundary conditions on the electric and magnetic fields at both the left and the right boundaries of the shield. If a shield has a thickness that is much greater than the skin depth, δ, at the frequency of the incident wave, this ratio is, [3]

$$SE = \frac{\hat{E}_i}{\hat{E}_t} = \frac{\left(\eta_0 + \hat{\eta}\right)^2}{4\eta_0\,\hat{\eta}}\left[1 - \left(\frac{\eta_0 - \hat{\eta}}{\eta_0 + \hat{\eta}}\right)^2 e^{-2t/\delta} e^{-j2\beta t}\right] e^{t/\delta} e^{j\beta t} e^{-j\beta_0 t} \quad (5.1)$$

Expressed in dB, the *magnitude* of the shielding effectiveness, SE_{dB}, becomes

$$SE_{dB} = 20\log_{10}\left|\frac{\hat{E}_i}{\hat{E}_t}\right| = \underbrace{20\log_{10}\left|\frac{\left(\eta_0 + \hat{\eta}\right)^2}{4\eta_0\,\hat{\eta}}\right|}_{R_{dB}} + \underbrace{20\log_{10} e^{t/\delta}}_{A_{dB}} + \underbrace{20\log_{10}\left|1 - \left(\frac{\eta_0 - \hat{\eta}}{\eta_0 + \hat{\eta}}\right)^2 e^{-2t/\delta} e^{-j2\beta t}\right|}_{M_{dB}} \quad (5.2)$$

or, concisely, in terms of the reflection, absorption, and multiple reflection losses:

$$SE_{dB} = R_{dB} + A_{dB} + M_{dB} \quad (5.3)$$

It is very important to point out that this solution was obtained under the assumption of a uniform plane wave, i.e., when the shield is in the *far field* of the source. Since, in the far field, the magnitudes of the electric and magnetic fields are related by a constant, the shielding effectiveness for the magnetic field is exactly the same as the one for the electric field (unlike the case of the near-field shielding). The result shown in *Eq. (5.2)* greatly simplifies under the assumption of a thick shield made up of a good conductor. The multiple reflection loss can be ignored and the reflection and absorption losses become, [3]

$$R_{dB} = 20\log_{10}\left|\frac{\eta_0}{4\,\hat{\eta}}\right| \quad (5.4a)$$

$$A_{dB} = 20\log_{10} e^{t/\delta} \quad (5.4b)$$

Thus, a reasonable, far-field approximation for the shielding effectiveness of a thick, good conductor is

$$SE_{dB} = R_{dB} + A_{dB} \quad (5.5)$$

with the reflection and absorption losses given by *Eqs. (5.4)*. The reflection loss in *Eq. (5.4a)* can be equivalently expressed as, [2]

$$R_{dB} = 168 + 10\log\left(\frac{\sigma_r}{f\mu_r}\right) \quad (5.6)$$

Evaluating the logarithm in *Eq. (5.4b)* and expressing the thickness in inches, the absorption loss can be equivalently expressed as

$$A_{dB} = 3.34t\sqrt{f\mu_r\sigma_r} \quad (5.7)$$

Section 6 – Near-Field Shielding

The distinction between electric and magnetic field sources allows us to use the results of the previous section and the far field shielding to obtain the approximate formulas for the near field shielding.

Recall *Eq. (5.4a)*, repeated here, for the reflection loss in the far field

$$R_{dB} = 20\log_{10}\left|\frac{\eta_0}{4\,\hat{\eta}}\right| \quad (6.1)$$

The reflection loss for the near-field electric sources is obtained by substituting the wave impedance from *Eq. (4.5)* for the intrinsic impedance of free space in *Eq. (6.1)*. The result is [2], [3]

$$R_{e,dB} = 322 + 10\log_{10}\left(\frac{\sigma_r}{\mu_r f^3 r^2}\right) \quad (6.2)$$

The reflection loss for the near-field magnetic sources is obtained by substituting the wave impedance from *Eq. (4.7)* for the intrinsic impedance of free space in *Eq. (6.1)*. The result is

$$R_{m,dB} = 14.57 + 10\log_{10}\left(\frac{fr^2\sigma_r}{\mu_r}\right) \quad (6.3)$$

The absorption loss in the near field is given by the same expression as that in the far field, i.e.,

$$A_{dB} = 20\log_{10} e^{t/\delta} \quad (6.4a)$$

or

$$A_{dB} = 3.34t\sqrt{f\mu_r\sigma_r} \quad (6.4b)$$

with the shield thickness, t, specified in inches. As was the case in the far field, the total shielding effectiveness in the near field is the sum of the reflection and absorption losses

$$SE_{dB} = R_{dB} + A_{dB} \quad (6.5)$$

Section 7 – Near-Field Shielding – Measurement Set Up

To verify the theoretical results in the near field we used two different circuits as electric and magnetic field sources and utilized four different solid shields, described in *Table 7.1*.

Table 7.1 Shield Configurations			
Material	Thickness (inches)	Relative Permeability, μ_r	Relative Conductivity, σ_r
Phosphor Bronze	0.008	1	0.15
Phosphor Bronze	0.015	1	0.15
Nickel Silver	0.008	1	0.058
Carbon Steel	0.008	100	0.106

The magnetic field source was a 9V to 5V step-down SMPS operating at a frequency of 125 kHz Measurements were taken from 100 kHz to 20 MHz with a near-field magnetic probe. The measurement setup and the circuit block diagram are shown in *Fig. 7.1*.

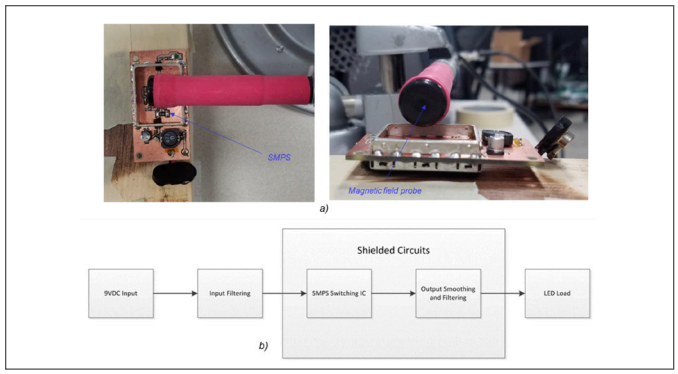

Figure 7.1: Magnetic source circuit – a) measurement setup, b) block diagram

The electric field was generated by a simple 1 MHz crystal oscillator. The crystal output was a 5V logic level signal into a 300 ohm resistor. Measurements were taken from 1 MHz to 900 MHz with a near-field electric probe. The measurement setup and the circuit block diagram are shown in *Fig. 7.2*.

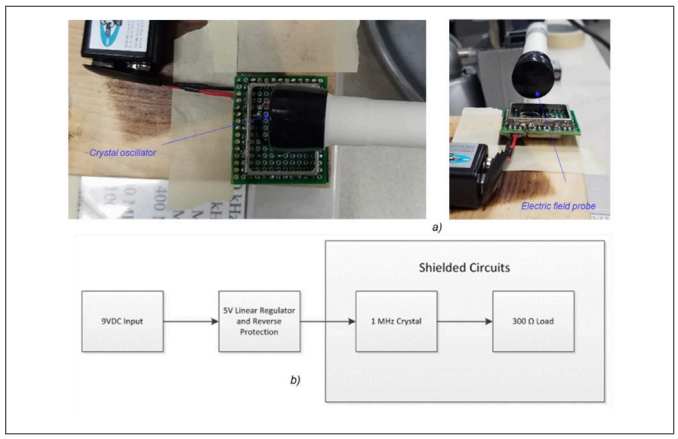

Figure 7.2: Electric source circuit – a) measurement setup, b) block diagram

Several measurements were taken for each source: a baseline with no shield present, and sweeps with each of the four different shield configurations.

In both measurement setups, the shield was at a distance of 5 mm from the source. To determine whether this distance could be considered as corresponding to the near-field, the expression in *Eq. (3.3a)* was examined as follows.

$$\beta r = \frac{2\pi}{\lambda_0} r = \frac{2\pi}{\frac{v_0}{f}} r = \frac{2\pi f}{v_0} r \qquad (7.1)$$

In the very near field we have, □□ □ 1, or

$$\frac{2\pi f}{v_0} r << 1 \qquad (7.2)$$

If we assume two orders of magnitude relationship in the above inequality, then we have

$$\frac{2\pi f}{v_0} r = 0.01 \qquad (7.3)$$

From *Eq. (7.4)* we can determine the highest frequency up to which the physical distance of 5 mm corresponds to the point in the very near field.

$$f = \frac{10^{-2} v_0}{2\pi r} \cong \frac{(10^{-2})(3\times10^{8})}{6\times5\times10^{-3}} = 10^{8}\ Hz \qquad (7.4)$$

This result means that up to the frequency of 100 MHz it is reasonable to assume that the shield is in the very near field of the source.

Section 8 – Near-Field Shielding – Simulation and Measurement Results

Phosphor Bronze – 8 mil vs. 15 mil thick

The simulated results for the magnetic field shielding (based on *Eqs. (6.3 - 6.5)* for the reflection loss, the absorption and the total loss are shown in *Fig. 8.1*.

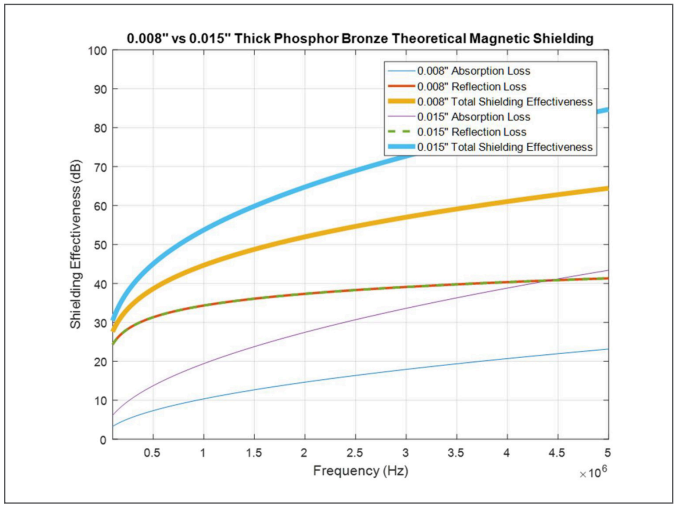

Figure 8.1: Phosphor bronze - 8 vs.15 mils: absorption, reflection, and total magnetic field loss

The reflection loss is the same for both shields but the absorption loss is larger for the thicker shield. Thus, the total shielding effectiveness of the 15-mil thick shield is larger than that of the 8-mil thick shield. The magnetic field measurement results for the two shields are shown in *Fig. 8.2*

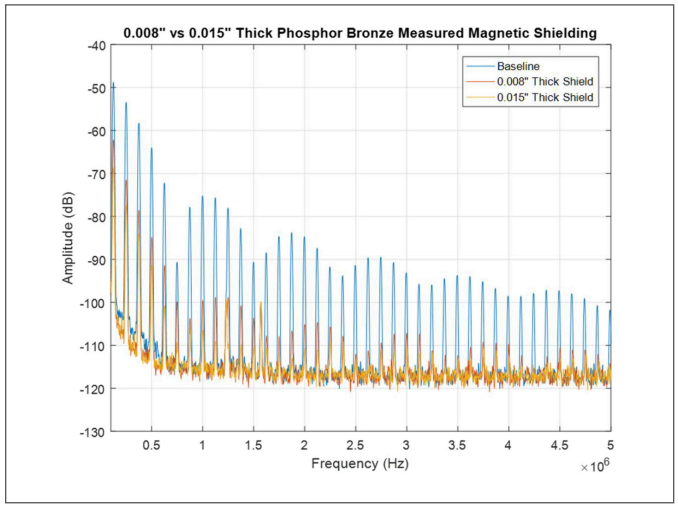

Figure 8.2: 8 mil vs. 15 mil phosphorus bronze – measured magnetic field

Increasing the thickness of the shielding material from 8 to 15 mils provided an additional 7 dB of shielding effectiveness at the fundamental operating frequency as well as 5-7 dB more shielding effectiveness between the 2nd and 10th harmonic. The measured results are consistent with the predictions of the theoretical formulas and the simulated results. Similar results were obtained by Adamczyk, and are presented in [4].

Next, let's look at the shielding effectiveness against the electric field.The reflection loss is specified by *Eq. (6.2)*; the absorption loss is the same as for the magnetic field and is specified by *Eq. (6.4)*. The simulated results for the *electric field* shielding for the reflection loss, the absorption and the total loss are shown in *Fig. 8.3*.

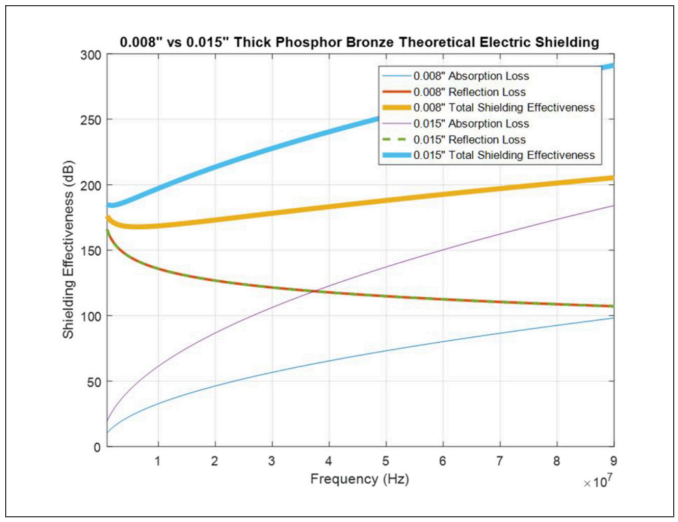

Figure 8.3: Phosphor bronze - 8 vs.15 mils: absorption, reflection, and total electric field loss

Again, the reflection loss is the same for both shields but the absorption loss is larger for the thicker shield. Thus, the total shielding effectiveness, against the electric field, of the 15-mil thick shield is larger than that of the 8-mil thick shield.

The electric field measurement results for the two shields are shown in *Fig. 8.4*.

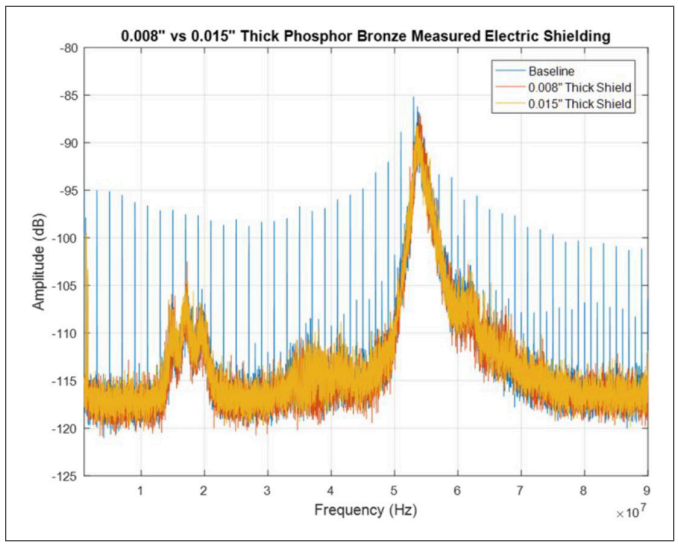

Figure 8.4: Phosphor bronze - 8 vs.15 mils: measured electric field

Since the raw measurements are hard to distinguish, let's look at their envelopes, shown in *Fig. 8.5*

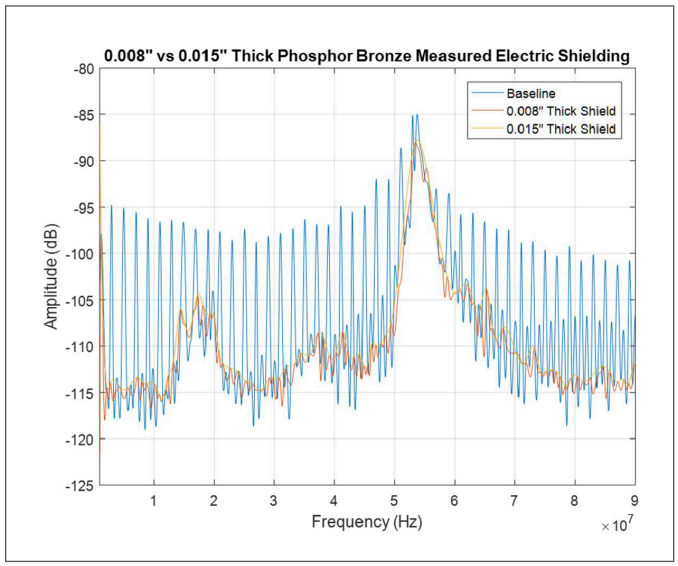

Figure 8.5: Phosphor bronze - 8 vs.15 mils: envelope of the measured electric field

It is apparent that both shields have a dramatic and similar effect on shielding against the electric field. While the theoretical formulas predict a significant difference in performance, especially at high frequencies, the measured results do not show this. (Note: the two broadband peaks, around 18 MHz and 53 MHz are due to the ambient noise present in the lab while performing the measurements).

The discrepancy can be explained by applying the theory discussed in *Section 2* that was developed for the far –field, ideal scenario. Recall, when the shield is in the far field, or equivalently, impinged by a plane wave, the electric field is greatly reflected, regardless of the thickness and the material of the shield (as long as it is a good conductor).

Our shield is in the near field, so why the results of the far field might apply here? The answer is that the near field results were developed under the assumption of an infinitely small (point) source, and the physical source of the actual emissions is definitely not small. Thus, it is conceivable that some of the electric field lines are perpendicular to the shield, and thus the far –field theory (where the impinging field is normal to the shield) is applicable.

We will observe very similar results for the electric field measurements for all other shields discussed in this paper.

Phosphor Bronze – Nickel Silver – Carbon Steel – all 8 mil thick

The simulated results for the total magnetic loss for each shield are shown in *Fig. 8.6*.

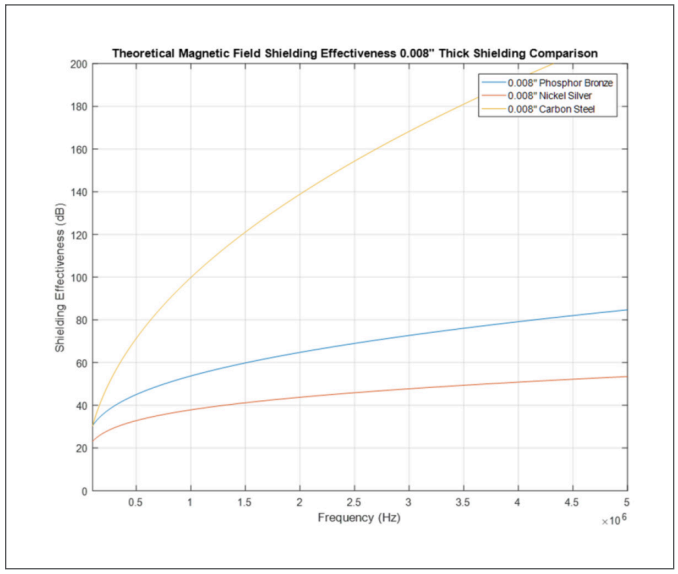

Figure 8.6: Different 8 mil shields - simulated total magnetic shielding effectiveness

The carbon steel shield clearly outperforms the other two shields, while phosphor bronze slightly outperforms nickel silver. The measured results are shown in *Fig. 8.7*.

Note that the measured results are consistent with the predicted simulated results. The carbon steel outperforms the other two shields, and phosphor bronze outperforms nickel silver. The carbon steel shield provides 25 dB of shielding effectiveness (vs. baseline) at the fundamental operating frequency as well as 32-36 dB from the 2nd to 10th harmonic was measured. This is due to the high absorption loss of the material which is made possible by having a relative permeability of 100.

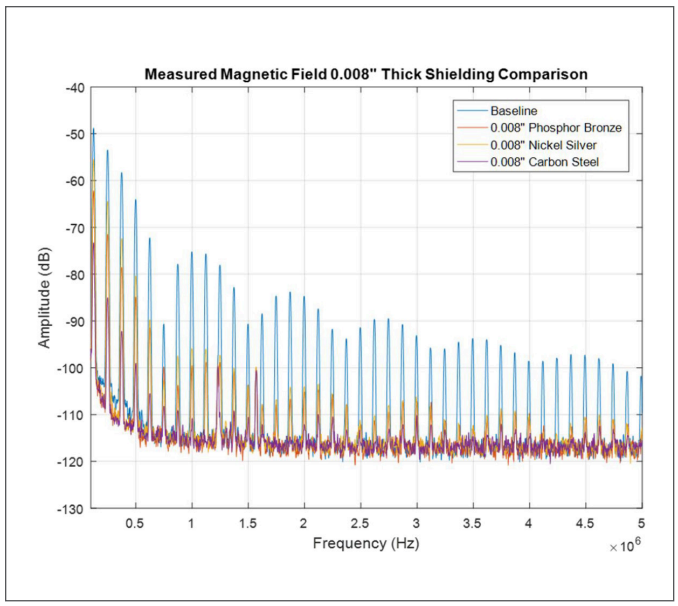

Figure 8.7: Different 8 mil shields - measured magnetic field

The relative permeability of phosphorus bronze is the same as that of nickel silver. The relative conductivity of phosphorus bronze, however is higher that of nickel silver. Thus, both the reflection loss and the absorption loss of phosphor bronzer is higher. The measurement results confirm these conclusions.

Nickel silver shield provided only a 5 dB shielding effectiveness at the fundamental and 14-22 dB between the 2nd and 10th harmonics.

Next, let's look at the shielding effectiveness against the electric field. The simulation results for the total loss for each shield are shown in *Fig. 8.8*.

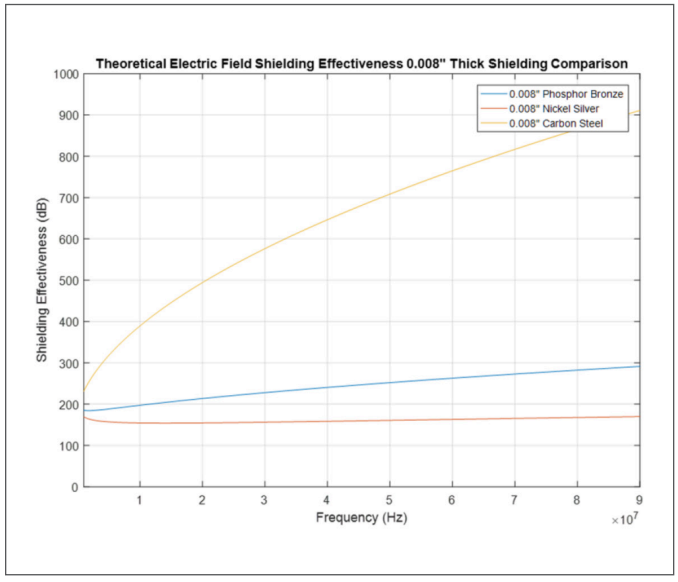

Figure 8.8: Different 8 mil shields - simulated total electric shielding effectiveness

The electric field measurement results for the three 8-mil shields are shown in *Fig. 8.9*.

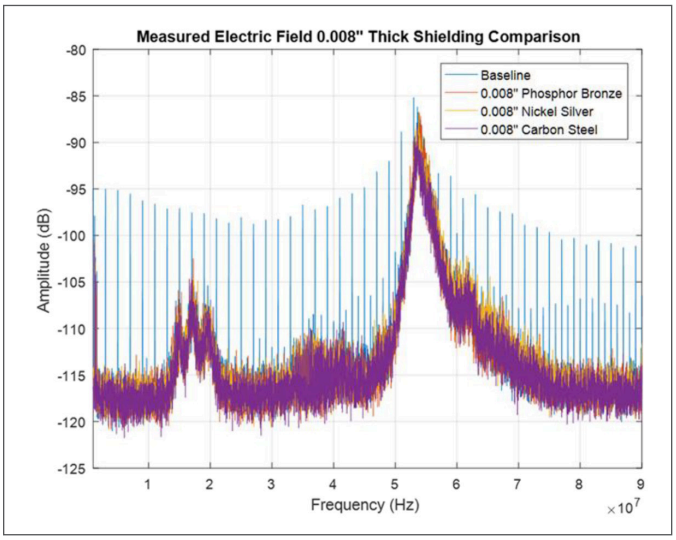

Figure 8.9: Different 8 mil shields - measured electric field

Again, an additional insight into the results is gained when looking at the envelopes of the measurements, shown in *Fig. 8.10*.

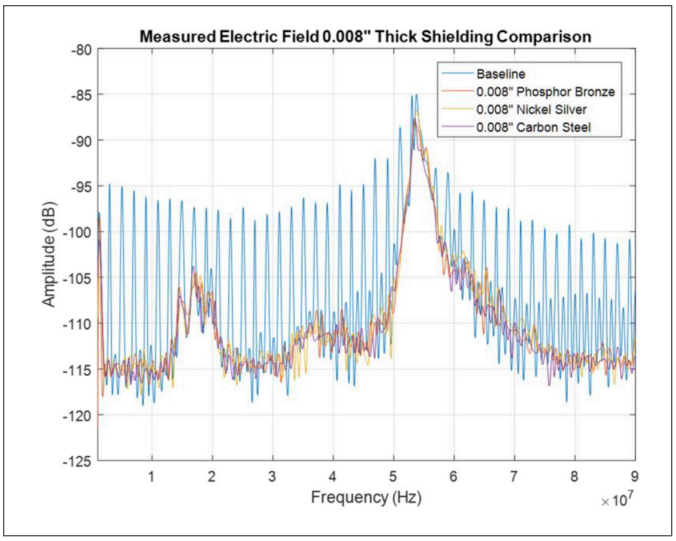

Figure 8.10: Different 8 mil shields - measured total electric shielding effectiveness

All shields have a dramatic and similar effect on shielding against the electric field. While the theoretical formulas predict significant differences in performance, especially at high frequencies, the measured results do not show this. This behavior can explained in the same manner as presented earlier for the 8 and 15 mil thick phosphor bronze shield.

Conclusions

This article presented the foundations of the shielding theory based on Schelkunoff's equations. The validity of these equations was assessed by performing the magnetic and electric field measurements in the near field of the source. It is shown that the H-field measurements in correlated with the results of Schelkunoff's equations; the E-field measurements however, did not.

The measurement results of the electric field in the near field of the source adhered to the wave theory developed for the far field. A plausible explanation of this fact was postulated: the shielding theory was developed under the assumption of a point source, which is not the case for practical sources in the near field of measurements.

References

[1] S. A. Schelkunoff, Electromagnetic Waves, Van Nostrand, 1943.
[2] Henry W. Ott, Electromagnetic Compatibility Engineering, Wiley, 2009.
[3] Clayton R. Paul, Introduction to Electromagnetic Compatibility, Wiley, 2006.
[4] Bogdan Adamczyk, Foundations of Electromagnetic Compatibility with Practical Applications, Wiley, 2017.

Author Bios

Dr. Bogdan Adamczyk is a professor and the director of the EMC Center at Grand Valley State University (http://www.gvsu.edu/emccenter/) where he performs EMC precompliance testing for industry and develops EMC educational material. Prof. Adamczyk has over 25 years combined industry and academia experience. He has taught numerous EMC certificate courses for industry. He is an iNARTE certified EMC Master Design Engineer, a founding member and the chair of the IEEE EMC West Michigan Chapter, and a member of the IEEE EMC Society Education Committee. He was a 2016 IEEE EMC Symposium Global University and Fundamentals of EMC instructor. He writes a monthly tutorial article for an EMC trade magazine. Prof. Adamczyk is the author of the textbook "Foundations of Electromagnetic Compatibility with Practical Applications" (Wiley, 2017). He can be reached at adamczyb@gvsu.edu

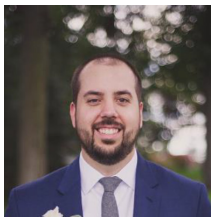

Nick Dipisa is a Senior EMC Engineer at Gentex Corporation where he helps facilitate the day-to-day operations of the EMC lab and performs test development activities. Before that role he worked as EMC Debug Engineer where he provided manufacturable and cost effective solutions to automotive EMC test failures. Nick graduated from Western Michigan University with Honors in 2011 with a BSEE and is currently enrolled as a graduate student at Grand Valley State University in their MSEE program. He may be reached at: nickdipisa@gmail.com

Need a Better Filter?

Ask a Curtis engineer for a better EMI filtering solution.

Curtis offers standard and custom solutions across a variety of applications and industries.

- Appliance
- Automotive
- Electronic
- Medical
- U.S. Military

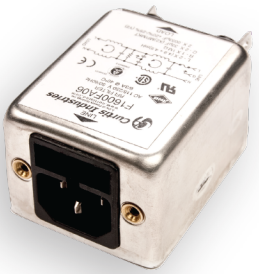

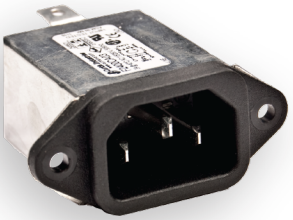

(800) 657-0853 • sales@CurtisInd.com

Innovative Engineering Solutions

CURTIS INDUSTRIES
A division of Powers Holdings, Inc.

www.CurtisInd.com/RFIFilters

USING COMMON MODE CHOKES IS NOT A KIND OF MAGIC

Lorandt Foelkel M.Eng.
Würth Elektronik eiSos GmbH & Co. KG
Lorandt.Foelkel@we-online.de

Introduction
Whenever electronic design engineers develop a power supply, at some point there will be a fight with Electro-Magnetic Compatibility (EMC). Reducing the Electromagnetic Interference (EMI) in switch mode power supplies (SMPS) can often be challenging because of the very high frequencies that are involved. In this frequency range, electronic components behave differently than expected as the parasitic effects of the components begin to play a dominant role. With this article, I describe some basics of low voltage buck converters from an EMI perspective, and provide some practical tips how to solve EMC in buck converter design.

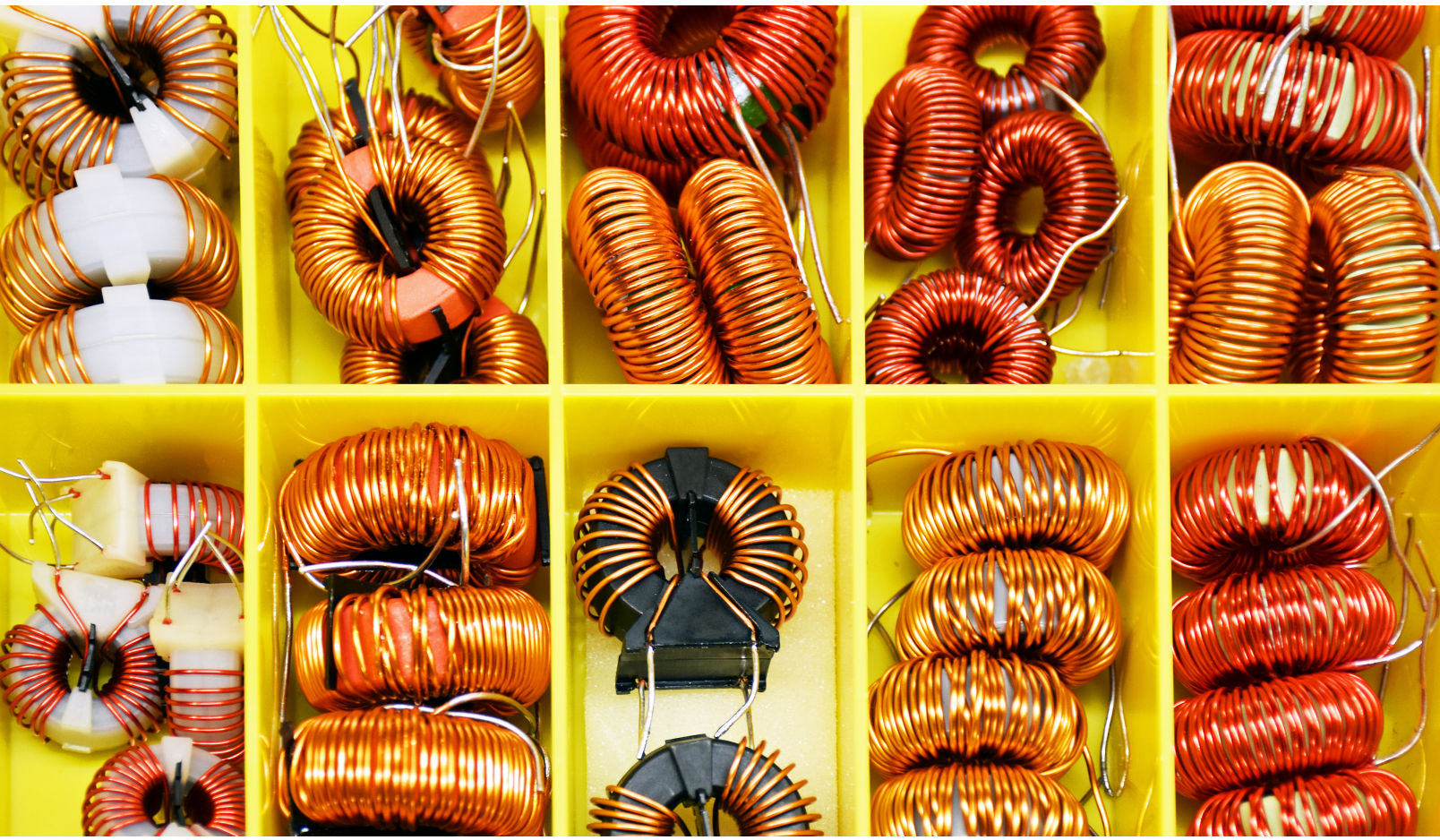

USING COMMON MODE CHOKES IS NOT A KIND OF MAGIC

When designing a SMPS, the EMC is often tested at the last stage of the design phase. If EMI has not been considered at the beginning of the design process, it can be very difficult and expensive to pass EMC tests. The best way to ensure a good and reliable EMC product design, is to consider the parasitics of components and follow a few simple EMI rules (design guides) at the beginning of the design. It is crucial that components are correctly selected and laid out to obtain good EMC results from the measurement laboratory.

EMI radiation can be generated by two sources:

- Alternating electric field source E (at high system impedance).
- Alternating magnetic field source H (at low system impedance).

Non-isolated DC/DC converters have relatively low impedance nodes and loops (much lower than the far-field impedance of 377 Ω), so magnetic fields are the main radiation sources in DC/DC buck converters. The current loop node will emit a high frequency magnetic field, which will gradually transit into an electromagnetic field when the distance to the source exceeds the reactive distance (λ/2*π).

From an EMI point of view, the current loop with the highest di/dt is the input area (“A” *Fig.1*) , which will generate the most high frequency interference and should be considered the most critical loop in buck converters. The di/dt of the current in output area (“B” *Fig.1*) is not as high as the input area (“A”) and normally generates less noise.

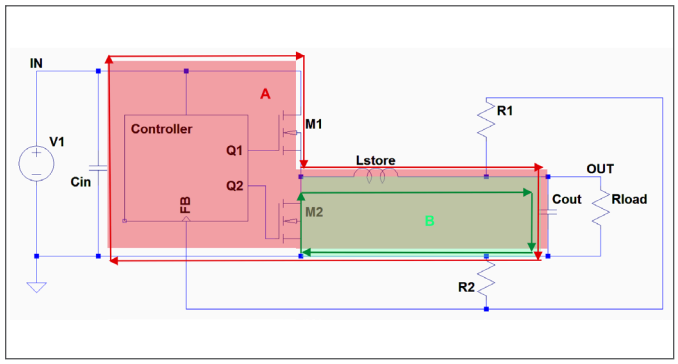

Figure 1 – The two primary current loops in a typical buck converter.

Theoretically, the input and output capacitors are considered ideal at very low impedance for the buck converter switching currents. Unfortunately, in real life, capacitors have ESR (Rs) and ESL (Ls), which increase capacitor impedance and result in extra high frequency voltage drops across the capacitors (*Fig.2*). This voltage will induce currents in the supply input line that also have parasitic inductance in addition to the output due the connections to the load.

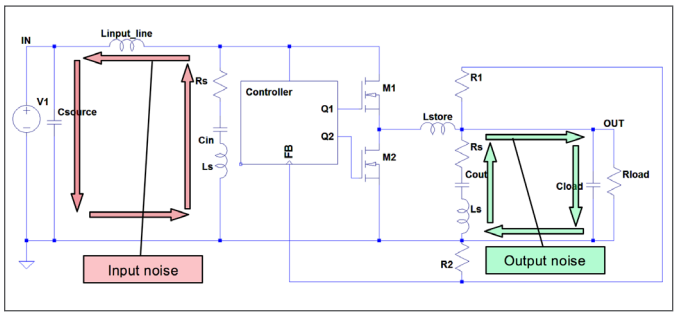

Figure 2 – The two current loops with parasitics shown.

Because of the discontinuous current flow at the buck converter input and the possibility of the supply lines to the DC/DC converter being quite long, the input can radiate considerably and can easily exceed the limits for conducted emission EMC measurements (150kHz ~ 30MHz).

To reduce the differential noise at the input, it is highly recommended to add an extra L-C filter in the input line (*Fig. 3*). When using pure inductance for Lfilter, it may be necessary to add one electrolytic capacitor Cbulk to dampen any input supply ringing and ensure stable input supply.

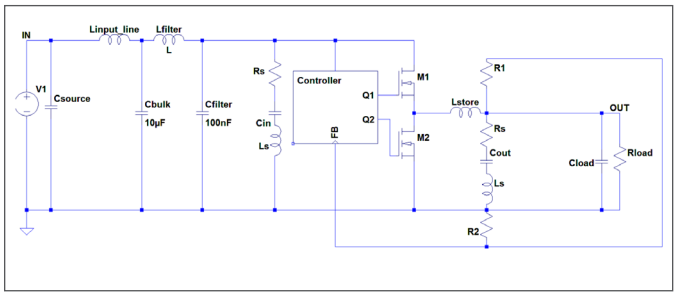

Figure 3 – Additional input filter added to reduce the differential noise.

A 1µH (ex. WE-PD2) or a Chip Bead Ferrite (ex. WE-CBF) with an impedance of 300 Ohm@100MHz can also be used for Lfilter. For Cbulk, it is recommended to use an Aluminum-Polymer Cap. The Cfilter should have a low ESR and low ESL limiting the selection to ceramic capacitors (MLCC).

This DC/DC buck converter can be considered a differential noise source and if not filtered sufficiently, can additionally generate common mode noise at all other I/O or even at the main power input.

The use of a common mode choke (CMC) is recommended for common mode noise filtering. These chokes can be manufactured in the same package with different core materials, such as NiZn or MnZn, and different winding structures, such as sectional or bifilar winding.

When the noise is higher in the MHz frequency region (>1 MHz) the right core material to attenuate in this bandwidth could be NiZn (*Fig.4* blue curve). If the noise is in the lower frequencies (<1 MHz), the right core material could be MnZn (*Fig.4* red curve).

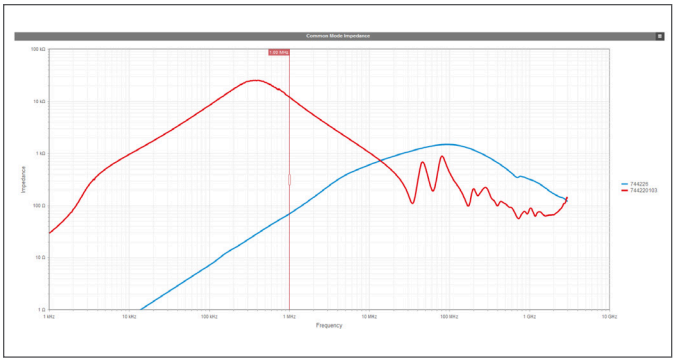

Figure 4 – Impedance curves suggested for frequencies above 1 MHz (NiZn in blue) or less than 1 MHz (MnZn in red).

Low inductance values where not many turns are needed, can be wound with different arrangements of the windings:

- sectors or
- bifilar

If the core material is the same and the number of turns is also the same, then the common impedance of those CMC's will be same. The big differences are the differential impedances (*Fig.5*).

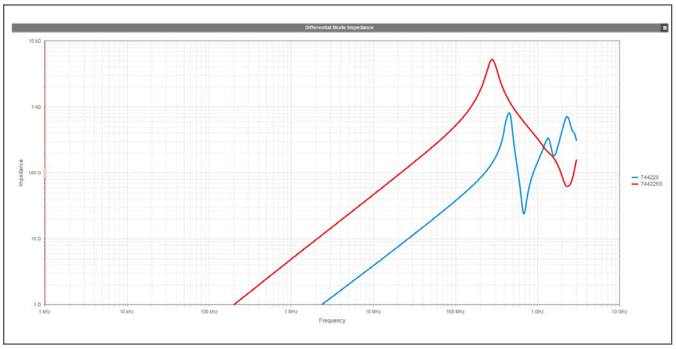

Figure 5 – Differential mode impedance curves for bifilar wound (blue) and sector wound (red)

This occurs because the leakage inductance of those CMC's is different. Where the bifilar winding (*Fig.6*) method has the lowest possible leakage inductance, the sector wounded (*Fig.7*) has the highest. The reason is the way the magnetic flux is compensated.

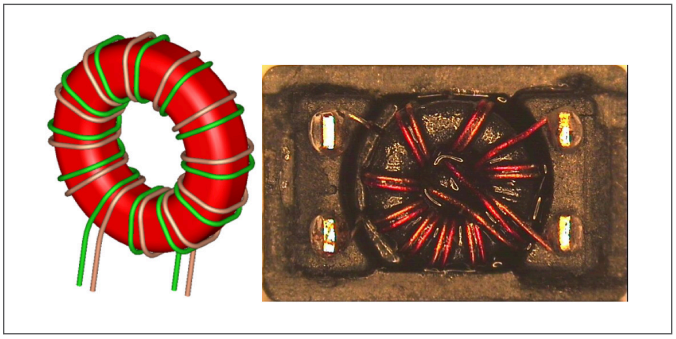

Figure 6 – A bifilar wound common mode choke.

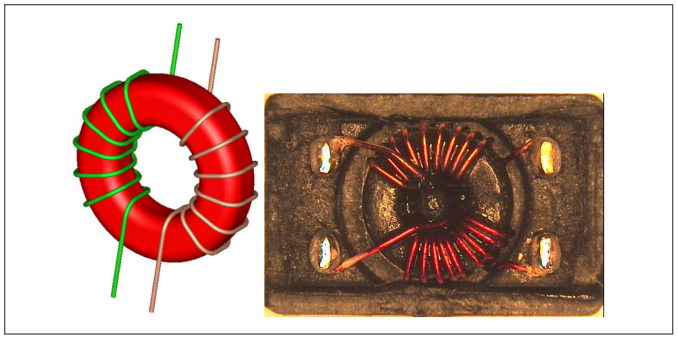

Figure 7 – A sector wound common mode choke.

There are some advantages and disadvantages depending on the application. A bifilar wound CMC has less differential impedance and in this way does not attenuate the main differential data signals and are excellent for higher speed signals like USB, CAN, etc., but have high capacitive coupling from line to line. The sector wound CMC has lower capacitive coupling but higher leakage inductance, making them unsuitable for high speed signals but excellent for filtering power supplies at inputs and outputs.

This characteristic can be seen in the free online tool **REDEXPERT** using the following link:
http://we-online.com/re/4nIfnTU0

In case the voltage exceeds 80 VDC from line to line, sector winding method must be used to fulfill the required creepage distance from safety regulations. The usage of TEX-E wire would be impossible to wind on such small cores.

The main advantages of sector wound CMC's are in fact the leakage inductance which can be used like a free add-on to filter differential noise. This leakage can be up to 5% of the main common mode inductance value. Adding two different values of X capacitors to the CMC, one before and one after the CMC, results in an excellent C-L-C Pi filter, where the leakage inductance decouples the two resonant points from the X caps.

Using such a filter topology for a buck or flyback converter helps to reduce input noise generated from DC/DC converters, and can avoid a costly redesign because of EMC test failure.

Author Bio
Lorandt Foelkel is the business development manager for energy harvesting and application engineer at Würth Elektronik eiSos GmbH for EMI/EMC and switched mode power supply (SMPS) design. He has provided more than 400 seminars on EMC and power supply design to engineers. He has over 29 years experience in electronic design, and has widespread experience for EMC and efficiency improvement for SMPS. He may be contacted at:
Lorandt.Foelkel@we-online.de

MEASURING SHIELDING EFFECTIVENESS WITH TWO NEAR FIELD PROBES

Kenneth Wyatt
Wyatt Technical Services LLC
ken@emc-seminars.com

Introduction

Sometimes you may find yourself needing to make a quick check on the shielding effectiveness (SE) of a material, such as plated plastic or shield gasket material. It's possible to set up a quick measurement setup using near field probes by using a couple H-field (for magnetic field SE) or E-field (for E-field SE). You'll also need a spectrum analyzer with tracking generator or network analyzer that covers the desired frequency range.

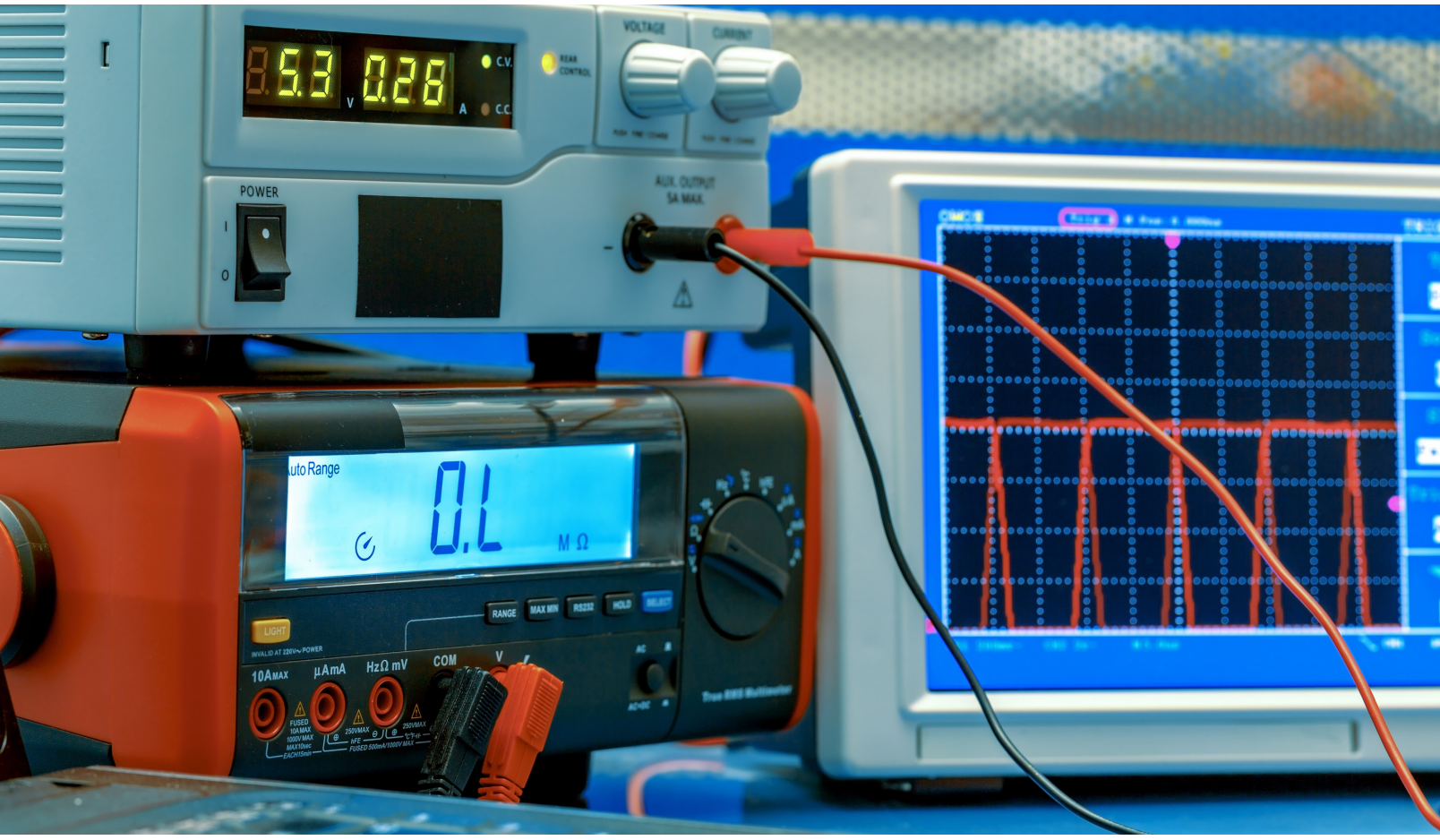

MEASURING SHIELDING EFFECTIVENESS WITH TWO NEAR FIELD PROBES

The use of two near field probes is not unique. In fact, I used this technique in the early 1990s to measure the SE of various plated plastics we were using at the time for oscilloscope enclosures during my time with Hewlett Packard. I even tried patenting the technique, but my lawyer discovered prior art. Both my colleagues, Doug Smith (http://www.emcesd.com) and Arturo Mediano (http://www.cartoontronics.com) have promoted this technique on their web sites and public seminars.

Measuring the SE in the near field is probably more pertinent for real products, because real enclosures are usually in the near field close to circuit boards. In fact, the results you get with this method won't agree with the far field SE equations (SE = A + R + M) one generally finds in the literature. George Kunkel wrote an article recently deriving the equations for near field SE using circuit theory as the basis. This is referenced below in [1].

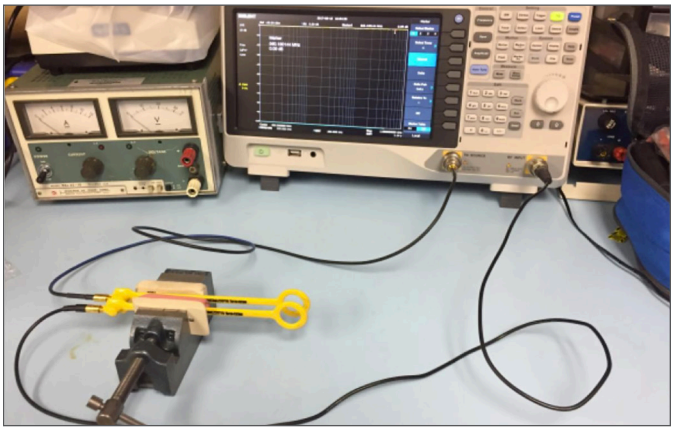

Figure 1 – The general test setup for the near field SE measurement.

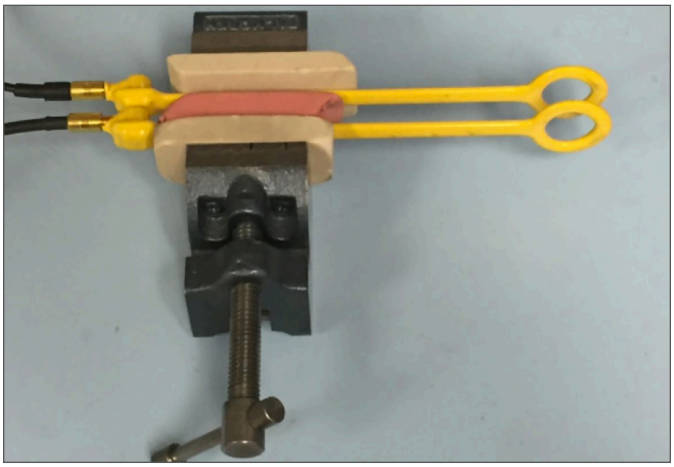

Figure 2 – Close-up of the two H-field probes in the vice. The erasers help isolate the probes from the metal of the vise.

For the purposes of this article, I'll be using a Siglent SSA3032X spectrum analyzer [2] with tracking generator and looking at frequencies in the range 1 to 1000 MHz. A pair of Beehive Electronics 100C H-field probes [3] were used. See *Figure 1* for the general test setup.

The probes were clamped between erasers in a small vise to hold them an arbitrary distance apart. The erasers helped isolate the probe shafts from the metal vise (*Figure 2*). The probe distance doesn't matter too much, except that they must be able to measure the sample without touching it and they must be close enough together to make a readable signal.

Connect one probe to the tracking generator output. Connect the other to the analyzer input. Try to separate the two coax cables to avoid coupling. Set up the spectrum analyzer as follows:

1. Start frequency = 1 MHz
2. Stop frequency = 1 GHz
3. Resolution bandwidth = 120 kHz (or 100 kHz) – not critical
4. Vertical scale = dBm
5. Reference Level = -20 dB
6. Preamp = Off
7. Attenuation = 0 dB
8. Tracking Generator (TG) = On (upper right on keyboard)
9. Tracking Generator Level = -20 dBm
10. In the TG menu, press Normalize
11. Turn TG = On

The SE response trace should appear in the top of the display and the top reference scale is now 0 dB. Placing any metallic sample between the probes will read out the SE directly versus frequency.

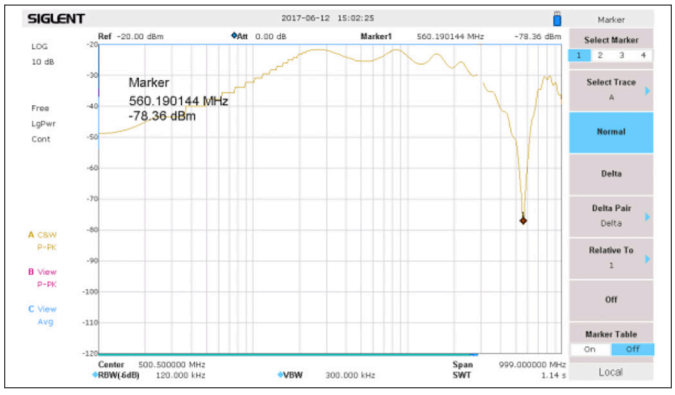

Figure 3 – A plot showing the 560 MHz resonance of the Beehive Electronics 100C probes used. While most of this is normalized out during the calibration procedure, still, some will remain and can be ignored in the displayed plots below

Note that the Beehive Electronics 100C probes I'm using have a sharp resonance about 560 MHz, which causes a spike in the response. I tried large paper clip loop probes and they exhibited a similar resonance. The use of the Beehive 100B (medium-sized) probes should move this resonance out of the displayed window. I didn't have a set of these, so had to use the larger probes as shown.

I'd just ignore the resonance and continue the SE plot straight through. See *Figure 3*.

Here are some sample measurements. See *Figures 4* through *9*.

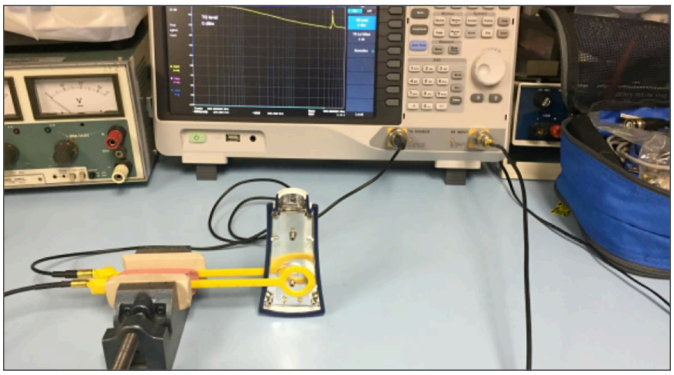

Figure 4 – A measurement of some typical plated plastic.

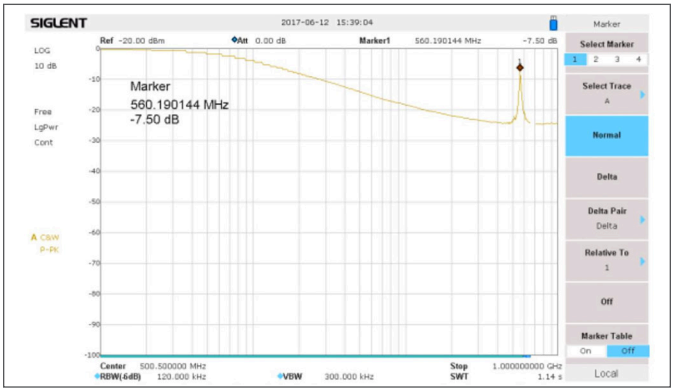

Figure 5 – Resulting plot for the plated plastic. Note it's only about 8 dB down at 20 MHz and 20 dB down at 100 MHz.

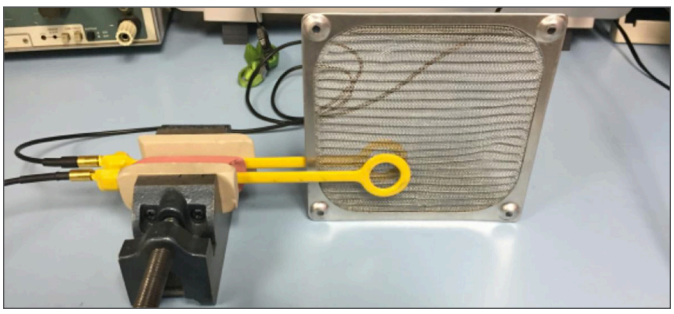

Figure 6 – A measurement of a fan EMI shield.

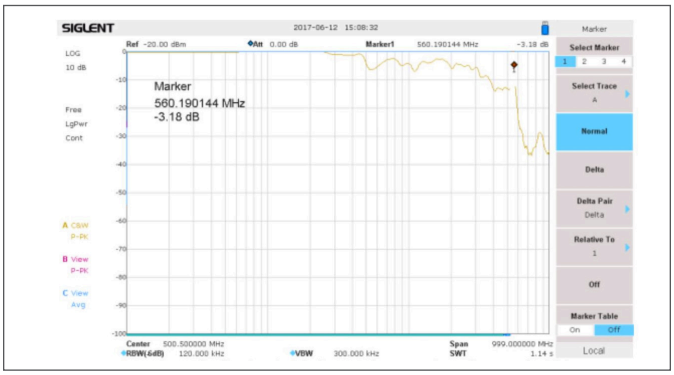

Figure 7 - Resulting plot for the plated plastic. This is a relatively poor shield for H-fields until you get above 600 MHz.

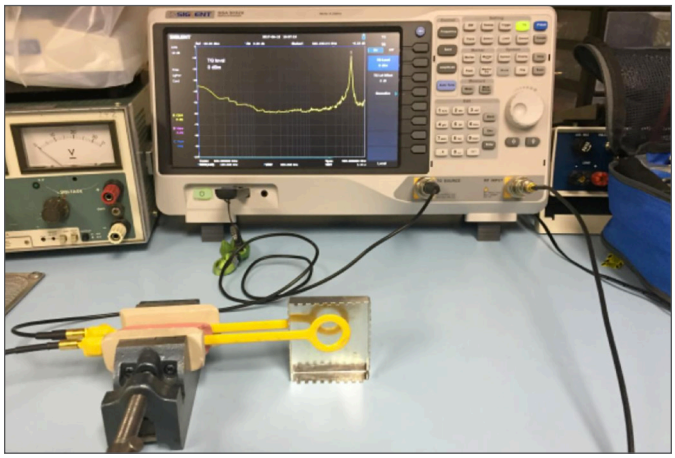

Figure 8 – A measurement of a solid steel local PC board shield.

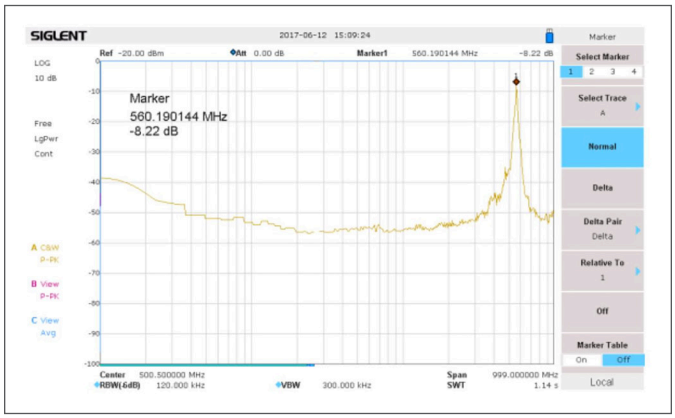

Figure 9 - Resulting plot for the plated plastic. Obviously, solid metal is much better than the thinner plated or screen shields. The SE averages about 50 dB throughout the frequency range.

Summary

Near field shielding effectiveness is easy to measure if you have a couple near field probes and either a spectrum analyzer or network analyzer. Plated plastics and most EMI gaskets or fan shields are inferior to solid metal.

References

[1] Kunkel, **A CIRCUIT THEORY APPROACH TO CALCULATING THE ATTENUATION OF SHIELDING BARRIERS**, Interference Technology, 2016 EMC Shielding Guide, Included in this issue of the 2017 EMI Shielding Guide.

[2] Siglent SSA3000X-series spectrum analyzer, http://siglentamerica.com/pdxx.aspx-?id=5113&T=2&tid=227

[3] Beehive Electronics 100C H-field probe, https://beehive-electronics.com/probes.html

MASTER SPONSOR

ROHDE&SCHWARZ

REGISTRATION IS OPEN!

2018 IEEE SYMPOSIUM ON ELECTROMAGNETIC COMPATIBILITY, SIGNAL AND POWER INTEGRITY

EMC+SIPI 2018

July 30 – August 3, 2018 Long Beach, CA

Your Port for EMC+SIPI Compliance

WE'RE ONLINE!

We continue our innovation for delivering top technical content featuring the Online EMC+SIPI.

Can't join us in-person?

Watch presentations ON DEMAND from the Symposium in Long Beach or your computer (or phone, or tablet!) Chat with other attendees, ask presenters questions, and learn the latest in EMC and signal & power integrity from anywhere. It's up to you how to attend!

EMC+SIPI 2018 Online is FREE to all 5-day Paid On-Site Technical Attendees

BENEFITS & FEATURES

www.emc2018usa.emcss.org

- Learn EMC, Signal Integrity and Power Integrity techniques
- Three days of expert technical papers
- Two full days of practical EMC+SIPI workshops and tutorials
- Experiments and demonstrations of fundamental and advanced topics
- Standards committee and working group meetings – observers are welcome to attend
- FREE Exhibit Hall! New Technologies, Instrumentation and Solutions from 150+ exhibitors
- Social networking, connecting, fantastic weather and an easy waterfront vibe

IEEE | EMC SOCIETY

EMI BASICS AND BOARD LEVEL SHIELDING DESIGN

Nick Demyanovich
Leader Tech Inc.
ndemyanovich@leadertechinc.com

Introduction

In today's world full of digital electronic devices, electromagnetic interference (EMI) is a major concern in both military and commercial marketplaces. Electrical equipment can become susceptible to these undesirable emissions and malfunction due to their presence. The simplest and most cost-effective method for reducing EMI is to first attack it at the board level if possible. Given the increasing complexity of circuitry these days, it is rare that a printed circuit board (PCB) layout can solve EMI problems entirely; thus board level shielding has become a requirement for most PCB designers.

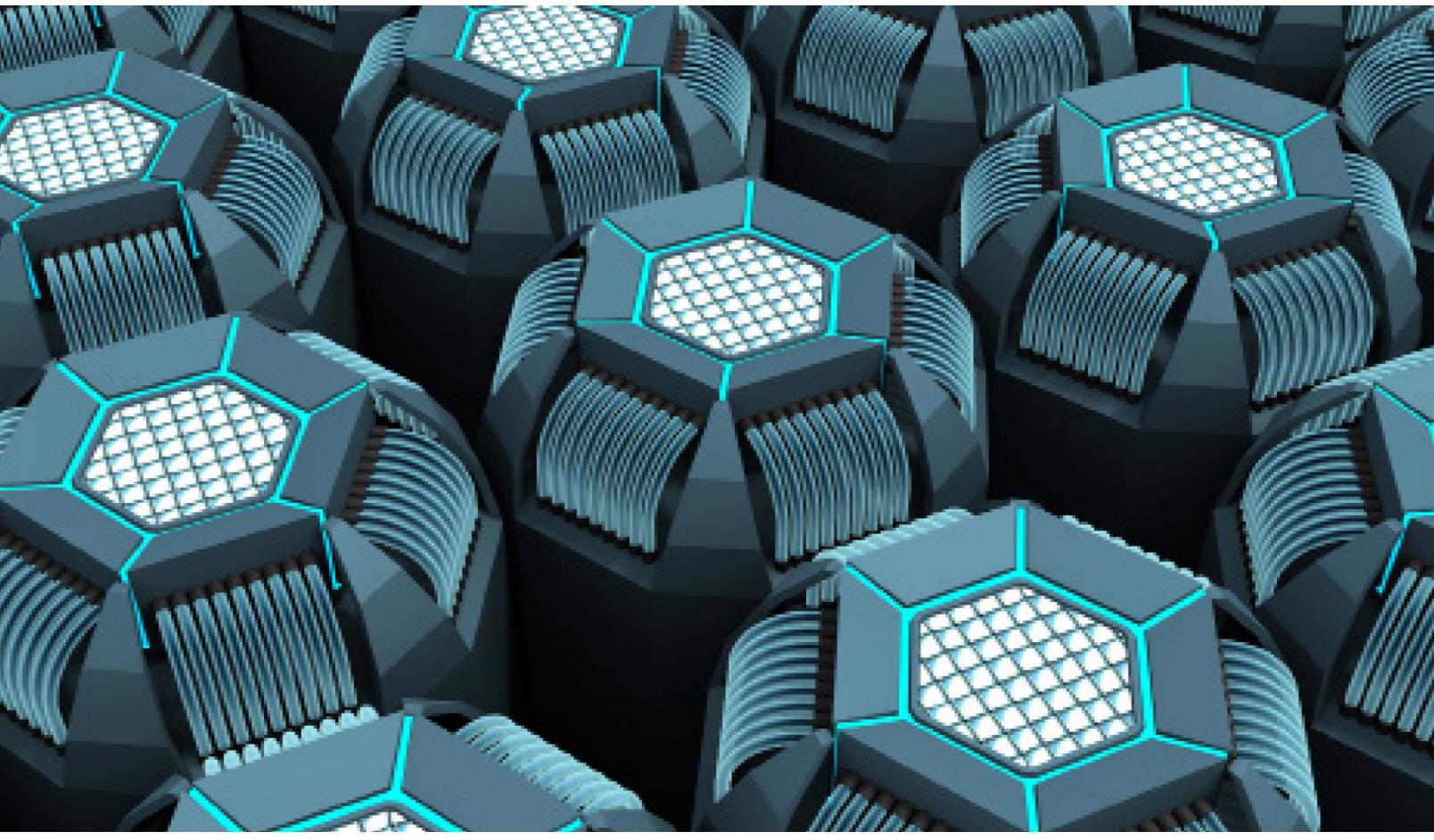

EMI BASICS AND BOARD LEVEL SHIELDING DESIGN

Radiated EMI occurs when an electromagnetic wave travels in the direction of an electronic device, and then disrupts the operation of that electrical component. An electromagnetic wave consists of an electric field (E) and a magnetic field (H), and the ratio of E to H (E/H) is known as the wave impedance (Z). For air or free space, Zo = 377 Ω. An electromagnetic wave with an impedance below this value is predominantly magnetic, whereas a wave with an impedance above it is mainly electric.

Using a board level shield for EMI shielding means to use a metal can, also known as a faraday cage, to enclose an electronic circuit on a PCB. This in turn will limit the amount of EMI radiation from the external environment that can disrupt PCB components, and also mitigate the amount of EMI energy generated by the circuit from escaping into the external environment.

The efficiency of a board level shield is measured in terms of shielding effectiveness (SE), which is the amount of EMI attenuation expressed in terms of decibels (dB). As depicted in *Figure 1* (Gnecco, 2000), when an electromagnetic wave comes in contact with the shield material, some of that energy is reflected, some is absorbed into the shield material, and some of it passes through the material. Thus, the total shielding effectiveness of an EMI shield is based upon the summation of the losses due to reflection and absorption.

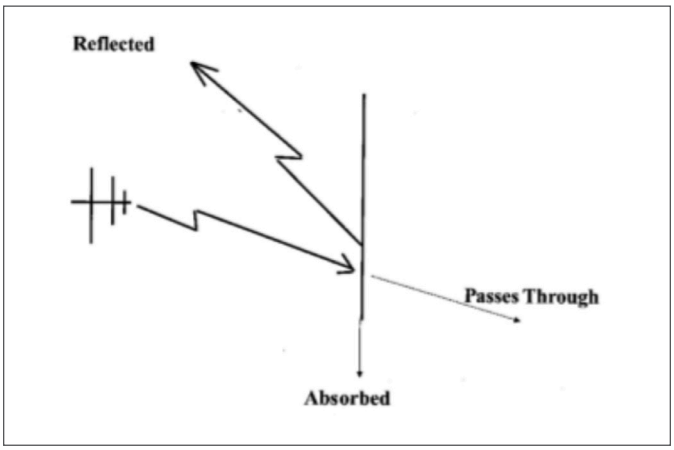

Figure 1 - Electromagnetic Wave at Shield Surface

Absorption loss is dependent upon the physical characteristics of the shield, and is directly proportional to the thickness of the shield, relative magnetic permeability and electrical conductivity of the material, and the frequency of the electromagnetic wave. Therefore, a thick walled shield with high permeability and conductivity will perform well in terms of absorption loss. Absorption loss is critical when emission suppression is needed, such as when a shield is being used to prevent electromagnetic energy from escaping an enclosure; see *Figure 2* (Tong, 2008).

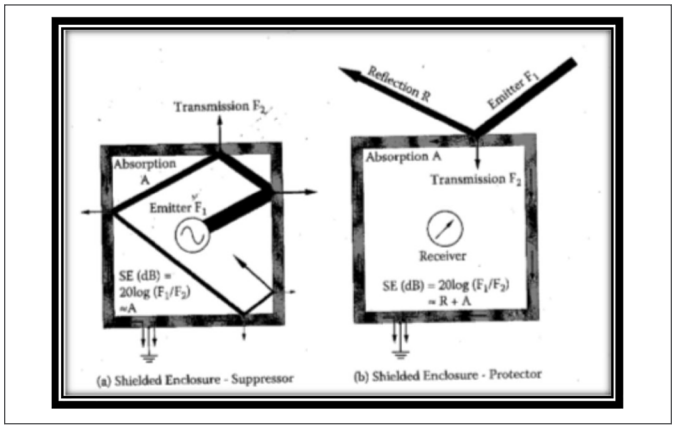

Figure 2 - EMI Protection vs. EMI Suppression (Tong, 2008)

On the other hand, reflection loss is important when a PCB component is to be protected from external sources. Reflection loss is dependent upon the relative mismatch between the impedance of the electromagnetic wave and that of the EMI shield material. If an electromagnetic wave's impedance differs from that of an EMI shield, then the wave will be partially reflected back. On the contrary, if the shield's and wave's impedance values are closely matched, then the energy will pass through the shield.

It is important to note that electrically dominant incident waves (impedance greater than 377 Ω) have high impedance, and higher conductive metals have low impedance. Thus, highly conductive metals exhibit high reflection loss for electrically dominant waves. However, for magnetically dominant incident waves that have low impedance (less than 377 Ω), the impedance mismatch between the shield & wave is minimal; hence the resulting reflection loss is very low. As a result, absorption loss is critical for shielding magnetic fields.

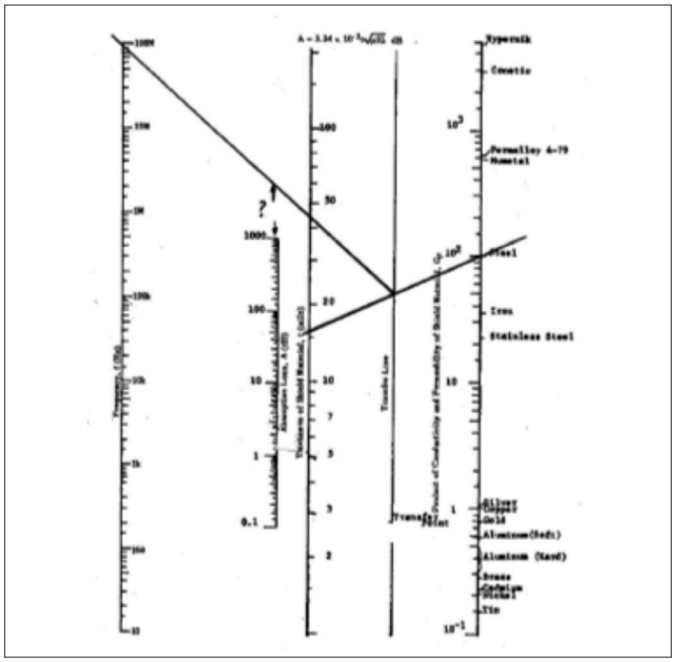

Figure 3: Absorption Loss w/ Material, Frequency & Shield Thickness

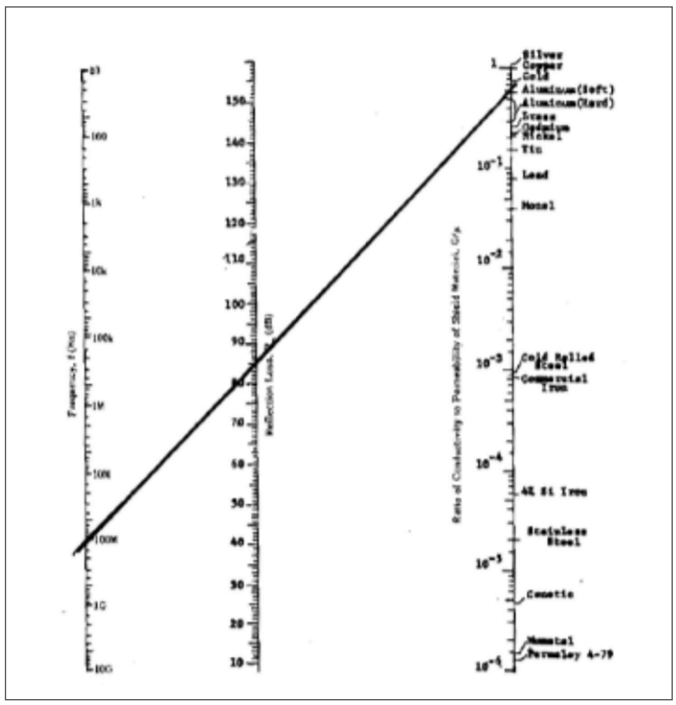

Figure 4: Reflection Loss w/ Material & Frequency (Gnecco, 2000)

Figures 3 and *4* (Gnecco, 2000) illustrate the theoretical absorption and reflection loss that can be achieved with an EMI shield using different materials, respectively. In order to make use of *Figure 3*, a line must be drawn from the known thickness of the EMI shield to the material being used, and then another line must be drawn from where it intersects the transfer line to the frequency of the incident electromagnetic wave. It is evident when viewing *Figure 3* that for a given frequency a thick walled shield with a high permeability material such as high permeability steel will outperform a thin walled highly conductive shield made of copper or brass in terms of absorption loss.

On the other hand, *Figure 4* reveals that for a given frequency highly conductive materials (copper or brass) will surpass the performance of a lesser electrically conductive material (high permeability steel or stainless steel) in terms of reflection loss.

Although conceptual tools such as *Figures 3* and *4* are helpful in determining the appropriate shielding material for a given application, it is not entirely realistic as they assume that no apertures are present in the shield design. The performance of EMI shields is greatly affected by seams and penetrations, especially when dealing with electrically dominant waves at higher frequencies.

The higher the frequency of an electromagnetic wave, the shorter its wavelength and the more likely it is to escape through any openings in an EMI shield. Therefore, when designing an enclosure it is critical to minimize the apertures to decrease the potential EMI leakage points, and to maximize the quality of the design near apertures for overall performance & reliability for the long term.

The frequency at which electromagnetic energy will propagate through an aperture without being attenuated is known as the cutoff frequency (fc). Frequencies above fc will propagate freely, while those below fc are attenuated. The equations below (Weibler, 1993) demonstrate how to calculate the cutoff frequency.

$f_c = c / \lambda_c$; where c is the speed of light (m/s), λ_c is the cutoff wavelength (m), f_c is the cutoff frequency (Hz)

For:

- Circular apertures: $\lambda_c = 3.412r$; where r = radius of the aperture (m);
- Rectangular apertures: $\lambda_c = 2a$; where a = longest dimension of the aperture (m)

Besides knowing the cutoff frequency, a good rule of thumb to achieve excellent EMI shielding effectiveness in any application is to keep every aperture size no larger than 1/20 wavelength of the electromagnetic wave being attenuated, and to aim for aperture sizes as small as 1/50 wavelength (Tong, 2008). *Table 1* below is a helpful resource that lists a sampling of frequencies and their corresponding wavelengths and recommended maximum aperture size based on 1/20 and 1/50 wavelength.

Table 1: Frequency-Wavelength Chart

Frequency (GHz)	Wavelength (mm)	1/20 Wavelength (mm)	1/50 Wavelength (mm)
0.5	600	30	12
1	300	15	6
2	250	12.5	5
3	100	5	2
4	75	3.75	1.5
5	60	3	1.2
10	30	1.5	0.6
20	15	0.75	0.3
50	6	0.3	0.12
100	3	0.15	0.06

Proper design of EMI board level shielding is crucial, and if done right can even eliminate the need for overall enclosure-level shielding. Many EMI shield manufacturers have fully tooled standard, low cost off-the-shelf options readily available. Therefore, it is a good idea to plan and design for the use of board level shields during the initial PCB design to take advantage of these options.

References

1. Gnecco, Louis T. 2000. The Design of Shielded Enclosures: Cost Effective Methods to Prevent EMI. Woburn, MA: Butterworth-Heinemann.
2. Tong, Xingcun Colin. 2008. Advanced Materials and Design for Electromagnetic Interference Shielding. Boca Raton, FL: CRC Press.
3. Weibler, Joseph. 1993. Properties of Metals Used for RF Shielding, EMC Test & Design.


ITEM MEDIA
Engineered Marketing For The Electronics Industry
Understand your customers' digital footprints to better understand their journey.
◦ Lead Qualification
◦ Lead Generation
◦ Audience Development
◦ Online Events
◦ Content Creation
◦ Technology Implementation
◦ Big Data Translation
◦ ...and MORE!
Start your journey today!
please visit
item.media
Additional ITEM Media Brands: Interference Technology | Electronics Cooling | Environmental Test & Design

GALVANIC CHART

Mike Oliver, VP Electrical Engineering
MAJR Products Corp.

Galvanic Chart

MIL-STD 1250A (Reference)		Gold	Graphite, Rhodium	Silver	Nickel, Monel	Copper, Bronze	Nickel silver	Stainless Steel	Brass	Chromium	Tin	Tin-lead solder	Lead	Iron, Steel	Aluminum	Cadmium	Galvanized steel	Hot-dip-zinc plate	Zinc	Magnesium
	Volt	0.15	0.05	0.00	-0.15	-0.20	-0.20	-0.20	-0.30	-0.45	-0.50	-0.50	-0.55	-0.70	-0.75	-0.80	-1.05	-1.05	-1.10	-1.60
Gold	0.15																			
Graphite, Rhodium	0.05	-0.10																		
Silver	0.00	-0.15	-0.05																	
Nickel, Monel	-0.15	-0.30	-0.20	-0.15																
Copper, Bronze	-0.20	-0.35	-0.25	-0.20	-0.05															
Nickel silver	-0.20	-0.35	-0.25	-0.20	-0.05	0.00														
Stainless Steel	-0.20	-0.35	-0.25	-0.20	-0.05	0.00	0.00													
Brass	-0.30	-0.45	-0.35	-0.30	-0.15	-0.10	-0.10	-0.10												
Chromium	-0.45	-0.60	-0.50	-0.45	-0.30	-0.25	-0.25	-0.25	-0.15											
Tin	-0.50	-0.65	-0.55	-0.50	-0.35	-0.30	-0.30	-0.30	-0.20	-0.05										
Tin-lead solder	-0.50	-0.65	-0.55	-0.50	-0.35	-0.30	-0.30	-0.30	-0.20	-0.05	0.00									
Lead	-0.55	-0.70	-0.60	-0.55	-0.40	-0.35	-0.35	-0.35	-0.25	-0.10	-0.05	-0.05								
Iron, Steel	-0.70	-0.85	-0.75	-0.70	-0.55	-0.50	-0.50	-0.50	-0.40	-0.25	-0.20	-0.20	-0.15							
Aluminum	-0.75	-0.90	-0.80	-0.75	-0.60	-0.55	-0.55	-0.55	-0.45	-0.30	-0.25	-0.25	-0.20	-0.05						
Cadmium	-0.80	-0.95	-0.85	-0.80	-0.65	-0.60	-0.60	-0.60	-0.50	-0.35	-0.30	-0.30	-0.25	-0.10	-0.05					
Galvanized steel	-1.05	-1.20	-1.10	-1.05	-0.90	-0.85	-0.85	-0.85	-0.75	-0.60	-0.55	-0.55	-0.50	-0.35	-0.30	-0.25				
Hot-dip-zinc plate	-1.05	-1.20	-1.10	-1.05	-0.90	-0.85	-0.85	-0.85	-0.75	-0.60	-0.55	-0.55	-0.50	-0.35	-0.30	-0.25	0.00			
Zinc	-1.10	-1.25	-1.15	-1.10	-0.95	-0.90	-0.90	-0.90	-0.80	-0.65	-0.60	-0.60	-0.55	-0.40	-0.35	-0.30	-0.05	-0.05		
Magnesium	-1.60	-1.75	-1.65	-1.60	-1.45	-1.40	-1.40	-1.40	-1.30	-1.15	-1.10	-1.10	-1.05	-0.90	-0.85	-0.80	-0.55	-0.55	-0.50	

Cathotic metals - least suseptable to corrosion (noble to less noble - vertical to horizontal)
Anodic metals - most suseptable to corrosion (less noble to noble - horizontal to vertical)

Green - Metals in harsh or marine environments such as salt spray or salt water. Volt potential difference equal or less than 0.15V
Blue - Metals in normal environments without temperature or humidity control, warehouse storage. Volt potential difference equal or less than 0.45V
Yellow - Metals in controlled environments with temperature and humidity control. Volt potential difference equal or less than 0.95V
Red - Not recommended


April 24 - 26, 2018
EMCLIVE 2018
ONLINE EVENT
Join industry leaders as they share and discuss the latest in EMI/ EMC technology. 3 days of practical, important and useful EMC information for electronics engineers. And it's FREE.
For more information about
Technical Presentations, Roundtables, Product Demos,
Whitepapers and Resources please visit:
emc.live
EMCLIVE 2018
Presented by
INTERFERENCE TECHNOLOGY

REFERENCES
(STANDARDS, ARTICLES, WHITE PAPERS, BOOKS, & LINKEDIN GROUPS)

SHIELDING EFFECTIVENESS TEST STANDARDS

Standard	Description
ASTM D4935-10	Standard Test Method for Measuring the Electromagnetic S hielding Effectiveness of Planar Materials
ASTM E 1851-15	Standard Test Method for Electromagnetic Shielding Effectiveness of Durable Rigid Wall Relocatable Structures
ASTM F3057-16	Standard Test Method for Electromagnetic Shielding Effectiveness of Glazings
ASTM WK41897	Electromagnetic Transmittance Rate of Glass or Glazing (Proposed)
IEC 60096-1	Replaced with IEC 60096-0-1, Radio frequency cables - Part 0-1: Guide to the design of detail specifications - Coaxial cables
IEEE 299:2006	IEEE Standard Method for Measuring the Effectiveness of Electromagnetic Shielding Enclosures
MIL-C-85485	Military Specification – Cable, Electric, Filter Line, Radio Frequency Absorptive
MIL-DTL-83528	Gasketing Material, Conductive, Shielding Gasket, electronic, Elastomer, EMI/RFI General specification
MIL-HDBK-1195	Military Handbook, Radio Frequency Shielded Enclosures
MIL-STD-188-125-1	DoD Interface Standard High-Altitude Electromagnetic Pulse (HEMP) Protection for Ground-Based C4I Facilities Performing Critical, Time-Urgent Missions
MIL-STD-285	Method of Attenuation Measurements for Enclosures and Electromagnetic Shielding, for Electronic Test Purposes
NSA 73-2A	Specification for Foil RF Shielded Enclosure (Tempest Protection for Facilities)
NSA 94-106	National Security Agency Specification for Shielded Enclosures
SAE ARP1705C	Coaxial Test Procedure to Measure the RF Shielding Characteristics of EMI Gasket Materials

ARTICLES AND WHITE PAPERS

1. Brull, Characterization of EMI Shielding Gaskets up to 40 GHz, Interference Technology, 2015 Europe EMC Guide.
2. Callen & Johnston, Stability of Nickel-Graphite Conductive Filler in Silicone Elastomer for EMI Shielding Applications, Interference Technology, May 2006.
3. Colotti, EMC Design Fundamentals, Telephonics, Presented at IEEE Long Island Section, EMC Society. 2005.
4. David, et al, On the characterization of electromagnetic shielding effectiveness of materials, Romanian Ministry of Education & Research, 2005.
5. Dexmet, Shielding Effectiveness of Expanded Metal Foils (EMFs), May 2017.Keebler, New Test Methods to Determine the Shielding Effectiveness of Small Enclosures Defined in IEEE P299.1, InCompliance, April 2011.
6. Fenical, The Basic Principles of Shielding, InCompliance, March 2014.
7. Fuerhaupter, Solving the Galvanic Corrosion Issue in EMI Shielding, Interference Technology, August 2008.
8. Inman, Shielding Effectiveness Measurement of EMI Gaskets and Flange Treatments Subjected to Salt Fog Exposure (20″ x 20″ Aperture), Chomerics, July 1992.
9. Fornes, New Techniques in Shielding for EMI, Interference Technology, 2014 Europe EMC Guide.
10. Krause, CONDUCTIVE CONCRETE FOR ELECTROMAGNETIC SHIELDING – METHODS FOR DEVELOPMENT AND EVALUATION, University of Nebraska, December 2012.Krieger Specialty Products, Radio Frequency Interference (RFI) Shielding Principles.
11. Mardiguan, Simple Method for Predicting a Cable Shielding Factor, Based on Transfer Impedance, Interference Technology, 2012 EMC Directory & Design Guide.
12. Perumalraj, et all, Electromagnetic Shielding tester For Conductive Textile Materials, Indian Journal of Fibre & Textile Research, December 2010.
13. Phipps & Keebler, Understanding Shielding Effectiveness of Materials and Measurements in the Near-Field and Far-Field, Interference Technology, May 2008.
14. She, Analysis on Shielding Effectiveness of Board Level Shielding with Apertures, Interference Technology, November 2013.
15. Vasquez, et al, Simple Device for Electromagnetic Interference Shielding Effectiveness Measurement, IEEE EMC Society Magazine, 2009
16. Wilson and Ma, A Study of Techniques for Measuring the Electromagnetic Shielding Effectiveness of Materials, NBS Technical Note 1095, 1986.

REFERENCES (CONTINUED)
(STANDARDS, ARTICLES, WHITE PAPERS, BOOKS, & LINKEDIN GROUPS)

RECOMMENDED BOOKS

1. Joffe and Lock, *Grounds For Grounding*, Wiley 2010
2. Morrison, *Grounding and Shielding - Circuits and Interference*, Wiley 2016
3. Ott, *Electronic Compatibility Engineering*, Wiley, 2009. A good general purpose text on EMC design, including shielding.
4. Paul, *Introduction to Electromagnetic Compatibility*, Wiley, 2006. The definitive upper level college textbook on EMC, including shielding.
5. Weston, *Electromagnetic Compatibility*, CRC Press, 2017. A good general purpose book on general EMC design, including shielding.

LINKEDIN GROUPS

- Electromagnetic Compatibility Forum
- EMC - Electromagnetic Compatibility
- EMC Experts
- EMC Testing and Compliance
- EMC Troubleshooters
- EMI and EMC Consultants
- Military EMC Forum

MAJOR EMC CONFERENCES

IEEE CONFERENCES (2017-2020)

2018 Joint IEEE International Symposium on EMC and APEMC
May 14-17
Singapore
Liu Enxiao, liuex@ihpc.a-star.edu.sg
Er Ping Li, erpingli@ieee.org
http://apemc.org

2018 IEEE Symposium on EMC, SI & PI
July 30-August 3
Long Beach, California
Ray Adams, r.k.adams@ieee.org
http://www.emc2018usa.emcss.org

2019 IEEE International Symposium on EMC, SI & PI
July 22-26
New Orleans, Louisiana
Dennis Lewis, dennis.m.lewis@boeing.com

2020 IEEE International Symposium on EMC, SI & PI
July 27-31
Reno, Nevada
Darryl Ray, darrylr16@yahoo.com

EUROPEAN EMC (AND RELATED) CONFERENCES (2017-2018)

EMV Conference
February 20-22, 2018
Düsseldorf, Germany
https://www.mesago.de/en/EMV/For_visitors/Welcome/index.htm

EMC Europe 2018
August 27-30, 2018
Amsterdam, The Netherlands
http://emceurope2018.org

INDEX OF ADVERTISERS

Coilcraft Inc.
1102 Silver Lake Road
Cary, IL USA 60013

t: (847) 639-6400
e: sales@coilcraft.com
w: www.coilcraft.com
page: 10

Curtis Industries
P.O. Box 343925
Milwaukee, WI

t: (800) 657-0853
e: sales@curtisind.com
w: www.curtisInd.com/RFI ilters
page: 21

EMC+SIPI 2018
2018 IEEE Symposium on Electromagnetic Compatibility, Signal and Power Integrity

Long Beach, CA & Online
July 30-August 3, 2018

w: www.emc2018usa.emcss.org
page: 28

ITG Electronics, Inc.
175 Clearbrook Road
Elmsford, NY 10523

t: (914) 806-8063
e: sales@ITG-electronics.com
w: www.ITG-Electronics.com
page: 4

SCHAFFNER EMC Inc
52 Mayfield Avenue
Edison, New Jersey 08837

t: +1-800-367-5566
e: usasales@schaffner.com
w: www.schaffnerusa.com
page: 2

Spira Manufacturing Corp.
650 Jessie Street
San Fernando CA 91340

t: (818) 764-8222
e: info@spira-emi.com
w: www.spira-emi.com
page: 7

EMC Live 2018
Online Event
April 24-26, 2018

w: emc.live
page: 35

ITEM Media
1000 Germantown Pike
Plymouth Meeting, PA 19462

t: (484) 688-0300
e: info@item.media
w: item.media
page: 32

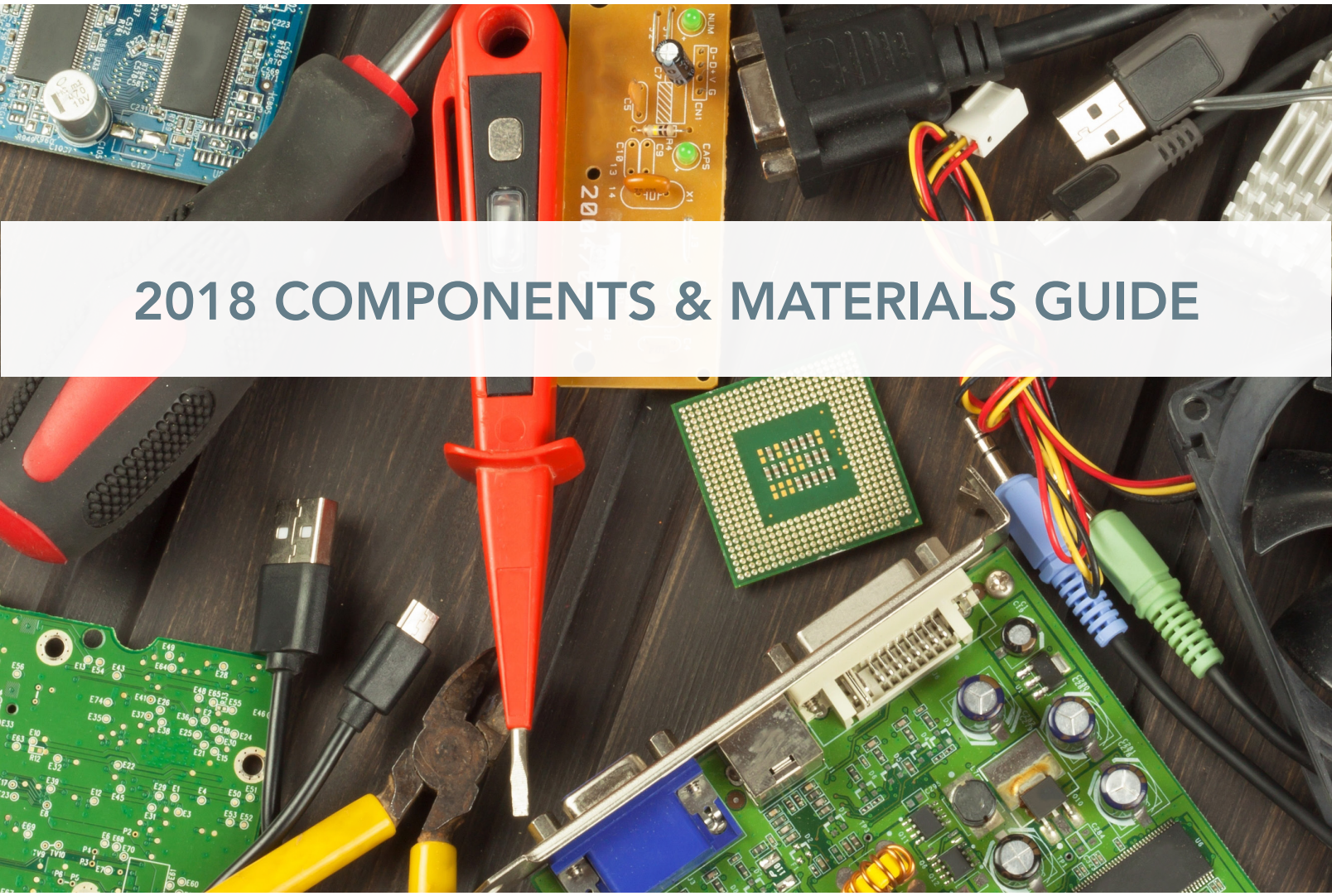

2018 COMPONENTS & MATERIALS GUIDE

INTERFERENCE TECHNOLOGY GUIDE SERIES
www.interferencetechnology.com